Evaluation of improved sea surface wind products from AMSR2 on GCOM-W

*Naoto Ebuchi[1]

1. Institute of Low Temperature Science, Hokkaido University

An improved version of the sea surface wind speed products (version 3 beta) from the Advanced Microwave Scanning Radiometer-2 (AMSR2) on the Global Change Observation Mission-W (GCOM-W) satellite were evaluated by comparisons with offshore moored buoy measurements, outputs from the European Centre for Medium-Range Weather Forecasts (ECMWF) Interim Reanalysis (ERA-Interim), and vector wind data from the RapidScat scatterometer (RSCAT) onboard the International Space Station (ISS). In general, the AMSR2 wind speeds agreed well with the reference data. The Root Mean Square (RMS) difference between the AMSR2 and buoy measurements was 1.13 m/s, which is close to the mission goal of 1 m/s. It is clearly exhibited that a systematic bias, which was discernible in the previous version (version 2.1) of the AMSR2 wind products, has been reduced in the latest version. Results of the triple collocation analysis suggest that the random errors in the AMSR2 version 3 wind speed are very close to 1 m/s and are smaller than those in the outputs from the numerical weather prediction (NWP) models, if random errors in the reference wind data (buoy, NWP, and RSCAT) are considered explicitly.

Keywords: AMSR2, GCOM, Microwave radiometer, Sea surface wind, Air-sea interation, Remote sensing

Validation and intercomparison for high resolution gridded product of surface wind vectors over the global ocean

*Kunio Kutsuwada[1], Hiroyuki Tomita[2], Shin'ichiro Kako[3], Tsutomu Hihara[4], Masahisa Kubota[1], Yu Takahashi[1]

1. School of Marine Science and Technology, Tokai University, 2. Nagoya University, 3. Kagoshima University, 4. JAMSTEC

Gridded products of surface wind vectors over the global ocean are constructed using multiple satellite data by microwave scatterometers and radiometers. Our new products, called the new version of the Japanese Ocean Flux data sets with Use of Remote-Sensing Observation (J-OFURO) V3, consist of various surface parameters such as sea surface temperature and specific humidity, and have temporal and spatial resolutions with daily mean and 0.25 x 0.25 degrees and cover a period from 1988 to the current. In our new procedure to derive gridded products of wind vectors with high resolutions, we combine data from microwave radiometers as well as scatterometers such as SSMI, AMSR-E, TMI, ERS-1,2, QuikSCAT, ASCAT. These gridded products are validated using our newly-designed quality control system (QCS) in which the reliabilities for various gridded products are examined by comparison with all available in-situ measurement data by moored buoys. Validations are also made by intercomparisons with other gridded products by single satellite (QSCAT and ASCAT), numerical model reanalysis (NRA-1, JRA55 and ERA-interim) and their combined "hybrid" (CCMP) products.
Results reveal that the J-OFURO3 product has relatively higher reliability than other satellite and reanalysis ones and lower than the hybrid one(CCMP), especially in the tropical Pacific region. Intercomparisons between the J-OFURO3 and CCMP exhibit noticeable spatial features in mean differences and correlations which are clearly dependent on buoy locations. This suggests that the CCMP product constructed by procedures including assimilation of buoy measurement data has inhomogeneous reliability in space, compared with our satellite-based product. Divergence and curl fields are derived from these gridded products of wind vectors, and similar spatial features are found in the tropical Pacific region.

Keywords: Wind vector, global ocean, multiple-satellite data

High Wind Observations within Extratropical Cyclones as Observed by Different Microwave Radiometers and Scatterometers

*Paul Chang[1], Zorana Jelenak[1], Faozi Said[1], Joseph Sienkiewicz[2]

1. NOAA/NESDIS/Center for Satellite Applications and Research, 2. NOAA/NWS/NCEP/Ocean Prediction Center

The validation of high wind speed measurements has proven to be extremely challenging due to the lack of surface truth, different sensor characteristics and their suitability for high wind observations, as well as different observation times. Because of this lack of surface truth, the forward models and geophysical model functions utilized in wind retrieval algorithms for different sensors are more often than not extrapolated and very hard to verify. Moreover, many high wind speed algorithms, especially from microwave radiometers, were developed with the goal of retrieving the extreme winds within tropical cyclones that would match aircraft-based high spatial resolution observations, even though the spatial resolution of the satellite observations is much coarser than that of both the aircraft-based measurements and measured physical phenomena. The implications have impact on both the operational use of high wind speed data as well as determining climatological trends and wind field characteristics.

Extratropical cyclones that reach hurricane force (HF) intensity are a significant threat to the safety of life at sea and a risk to cargo and vessels. Extratropical cyclones vary on scales from less than 100 km in diameter up to 4,000 km in diameter and have an average life cycle of five days from genesis to death. Associated wind conditions can range from light (10 to 20 knots), near gale (25 to 32 knots) gale force (33 to 47 knots), storm force (48 knots to 63 knots), or HF (greater than 63 knots). Knowledge of the wind structure, and in particular the frequency of occurrence and distribution of HF winds in extratropical cyclones has been greatly enhanced by data from the QuikSCAT scatterometer. Studies of the wind distribution within mature ETCs from the QuikSCAT scatterometer (cite our igarss paper) have shown there is more than a 20% probability of encountering gale force winds within 1000 km of the storm center at any time and direction for extratropical cyclones that reached the mature stage. The storm force winds can span beyond 1000 km from the storm center with the frequency decreasing significantly in the overall direction of motion. HF winds are concentrated within 1000 km radius west, south and southeast from the center relative to storm motion direction. Therefore, the spatial resolution of high winds within extratropical cyclones is suitable for all current radiometer and scatteroemter sensor observations. However, frequent observation of ETC's by the RapidScat and GPM sensors as well as the two ASCAT scatterometers have shown that high winds can change drastically over a 30 min time period. Therefore, any comparisons of wind retrievals by different sensors can be misleading and must be done carefully. To overcome this problem we compare composites of ETCs as obtained from wind observations from all radiometer and scatterometer different sensors.

To study the wind field distribution in these extreme ocean storm, composites of ocean surface wind speed fields were created by using a 50˚x 50˚ wide box that was divided into 400 lat/lon grid cells. This resulted in an approximate grid resolution of 12.5 km. The grid box was centered on the storm center locations obtained from Ocean Prediction Center best track storm file.

Keywords: extratropical cyclones, high winds, scatterometer, microwave radiometer

- ACG46-03 -

A Category '6' Trio –Supertyphoons Meranti (2016), Haiyan (2013), and Hurricane Patricia (2015)

*I-I Lin[1], M-M Lu[2], H.-C. Huang[1], J. Boucharel[3], F.-F. Jin[3], C.-C. Lien[1]

1. Department of Atmospheric Sciences, National Taiwan University, Taipei, Taiwan, 2. Central Weather Bureau, Taiwan, 3. University of Hawaii, USA

With peak intensity reaching 165 kts, supertyphoon Meranti was the most intense tropical cyclone on earth in 2016. Only 5 kts below the devastating super-typhoon Haiyan in 2013, Meranti was the 2nd most intense western Pacific typhoons on record. In ˜2.5 days, it rapidly intensified from category-1 to an impressive, category '6' (Lin et al. 2014; Lin et al. submitted 2017) intensity of 165 kts. Similar to Hurricane Patricia (185 kts, 2015, Huang et al. 2017) and Supertyphoon Haiyan (170kts, 2013), the peak intensity of these tropical cyclones are far above (30-50kts) the existing threshold (135 kts) of category-5 in the Saffir-Simpson scale. In addition, their intensity square (representing kinetic energy and a function of the Accumulated Cyclone Energy) is 140-180% higher than a 'regular' category 5 cyclone of 140kts. In terms of intensity cube (a function of the Power Dissipation Index), these extra-ordinary storms are 165-230% higher than a 140 kts category 5 cyclone (Lin et al. 2014; Lin et al. submitted 2017). This research highlights the importance of adding the new category '6' (165-185 kts) to the current Saffir-Simpson scale, for more accurate disaster mitigation and public awareness, because these category '6' TCs may carry much higher energy than regular category '5' TCs (e.g. other 140kts category 5s). In addition, they were all found to be associated with very favourable sea surface temperature (SST˜30C) and subsurface heat content conditions (˜120-140 kJ/cm^2.). This research further explores their interaction with ocean, as well as the oceanographic origin of these extremely favorable ocean conditions.

H.-C. Huang, J. Boucharel, I-I Lin*, Fei Fei Jin et al., Air-Sea Fluxes for Hurricane Patricia (2015): Comparison with Supertyphoon Haiyan (2013) and under Different ENSO Conditions, submitted, *J. Geophy. Res.*, 2017.
I-I Lin*, Mong-Ming Lu, et al., Taiwan in the hits of major typhoons, submitted, *BAMS*, State of Climate Report, 2017.
Lin I. I., I.-F. Pun, and Lien, C.-C. (2014) 'Category-6' supertyphoon Haiyan in global warming hiatus: contribution from subsurface ocean warming. *Geophys. Res. Lett,* doi:10.1002/2014GL061281.

Ocean Color from GCOM-C and Himawari-8

*Hiroshi Murakami[1]

1. Earth Observation Research Center, Japan Aerospace Exploration Agency

JAXA polar orbit satellite, Global Change Observation Mission for Climate (GCOM-C) which carries Second-generation Global Imager (SGLI) will be launched in 2017. SGLI will have 19 bands from near-UV (380 nm) to thermal infrared (12 um) wavelengths with 1150-km swath width. A key characteristic of SGLI for the ocean color observation is high spatial resolution (250 m). JMA geostational meteorological satellite, Himawari-8 has been in regular operation since July 7, 2015. Himawari-8 carries Advanced Himawari Imager (AHI) which has six spectral bands from visible to shortwave infrared wavelengths (470 nm, 510 nm, 640 nm, 856 nm, 1610 nm, and 2257 nm) with 500-m (640-nm band), 1-km (470, 510, and 856-nm bands), and 2-km (1610, and 2257-nm bands) spatial resolution.

Characteristics of the AHI for the ocean-color observation are high temporal resolution (10 min for the full-disk observation), small number of spectral bands, and relatively lower signal-noise-ratio (SNR) than general ocean-color sensors because the main target of AHI is meteorological observations. We have developed empirical ocean-color algorithms for SGLI and AHI spectral response (Murakami et al., OSJ 2015 fall meeting).

The SGLI 250-m spatial resolution can be advantage in monitoring of fine structures of coastal areas and front of currents, and detection of local phenomena such as red tide. However, they can change quickly and sometimes cannot be tracked by the temporal resolution of SGLI (once/2-day). Accuracy of ocean color estimate from instantaneous AHI measurements (every 10 min) is relatively worse due to the limited number of bands and low SNR. This study shows, however, the random noise can be reduced by averaging for about one hour (i.e., six scenes) when the 1- or 2-km scale phenomena can be assumed to be stable for an hour. Daily movement of front structures can be detected by the hourly AHI ocean color. Effective use of high spatial resolution data of the polar orbit satellite such as GCOM-C and high temporal resolution data of the geostationary orbit satellite such as Himawari-8 will be required in the next step.

Keywords: GCOM-C, SGLI, Himawari-8, Ocean color

Ocean color remote sensing of Chromophoric Dissolved Organic Materials (CDOM) for Second-generation GLobal Imager (SGLI) onboard the Global Change Observation Mission-Climate satellite (GCOM-C)

*Takafumi Hirata[1]

1. Faculty of Environmental Earth Science, Hokkaido University

Ocean is a large reservoir of the dissolved organic carbon on the Earth, storing approximately 38,000 PgC. Satellite observation methodologies have been developed by various researchers and space agencies and been offering a synoptic view of an optical proxy of the colored dissolved organic materials (CDOM) in the surface ocean on various temporal and spatial scales (e.g. from local and daily to global inter-annual scales). Second generation GLobal Imager (SGLI) onboard Global Change Observation Mission –Climate satellite (GCOM-C), to be launched by Japan Aerospace eXloration Agency (JAXA), also intends to measure CDOM in the surface ocean over the next several years, and a satellite algorithm for the new sensor was developed. The algorithm was based on a coupling of ocean colour inversions. One of the challenges in such inversion procedure has been to separate optically similar signals between CDOM and other detrital materials. Two empirical separations of these materials, different in terms of the degree of complexity in the algorithm, was tested. It was shown that a moderate complexity, rather than most simple nor complex, might give the best retrieval of CDOM under a current limitation in our ability to model every bio-optical processes.

Keywords: Ocean color, CDOM, SGLI, GCOM-C, remote sensing

Examples of Multi-Satellite Analyses for Advancing Earth System Science

*Michael H. Freilich[1]

1. NASA Headquarters

This presentation will describe NASA's current and planned Earth observing capabilities, the resulting science and applications,and NASA's long-standing partnership with Japan, with particular emphasis on the revolutionary use of multi-satellite heterogeneous and homogeneous constellations. NASA and the Japan Aerospace Exploration Agency (JAXA) have a long history of collaboration on satellite missions and are cooperating on several Earth observing constellations. NASA and JAXA have partnered for the last several years on calibration and validation activities associated with JAXA's Greenhouse Gases Observing Satellite (GOSAT) and NASA's Orbiting Carbon Observatory (OCO0-2) missions. And in 2012, JAXA's Global Change Observation Mission - Water (GCOM-W1) satellite joined Aqua and other NASA missions as part of the international Afternoon Constellation (A-Train). The results from these (and other) Earth observing missions are expanding our knowledge of the current state of the Earth system and our ability to predict how it may change in the future. These data also enable a wide range of practical applications that benefit society.

Keywords: TRMM, GPM, GOSAT, ASTER, AMSR-E, A-Train, Constellations, Small-Satellites, International Space Station

From Satellite Data to Informatics –Towards The Development of Satellite-based Real-Time Informatics in Community Satellite Processing Package (CSPP)

*Allen A Huang[1,2]

1. University of Wisconsin Madison, 2. SSEC/CIMSS

In cooperation with the United States National Oceanic and Atmospheric Administration (NOAA) and National Aeronautic and Space Administration (NASA), Cooperative Institute for Meteorological Satellite Studies (CIMSS) of Space Science and Engineering Center (SSEC) is continuing to develop NASA-supported International MODIS/AIRS Processing Package (IMAPP) and NOAA-funded Community Satellite Processing Package (CSPP). These community software packages are to provide both official and users developed algorithms and processing codes for the optimal and broad use of international polar orbiter satellite and geostationary satellite data collected from NOAA/NASA S-NPP, GOES-R, EUMETSAT METOP series, and Japanese Meteorological Administration (JMA) Advanced Himawari Imager (AHI).

This paper starts with the overview of ˜16 years (2000-2016) of success of IMAPP and CSPP as a pathway to the development of a freely available software package to transform MODIS, AIRS, AMSU, VIIRS, CrIS, and ATMS Raw Data Records (RDRs) (i.e. Level 0) to Sensor Data Records (SDRs) (i.e. Level 1), SDRs to Environmental Data Records (EDRs) (i.e. Level 2) and Information Data Record (IDRs) in support of Terra, Aqua, Suomi NPP and subsequently the JPSS and GOES missions under the CSPP framework.

Moreover, the current innovations in the development of Information Data Record (IDR) from single or multiple EDR and other ancillary and auxiliary data, to become the foundation of CSPP informatics. Examples of real-time applications using EDRs and IDRs in nowcasting and nearcasting of severe weather, aviation operation and air quality monitoring are to be highlighted. Summary is given to conclude this community effort in facilitating the user-friendly end-to-end calibration, navigation, product generation and information integration that are suitable and freely available to all users of meteorological and environmental satellites.

Keywords: Community satellite processing package, Sensor Data Record; Environmental Data Record; Information Data Record, Nowcasting; Nearcasting

Sustainable Development Goals (SDGs) and Earth observations-JAXA's activities for SDGs

*Chu Ishida[1]

1. Japan Space Exploration Agency

In adopting the 2030 Agenda for Sustainable Development in September 2015 at a High-level Political Forum on Sustainable Development, world leaders agreed that a global indicator framework was necessary to measure, monitor and report progress towards the 17 transformational Sustainable Development Goals (SDGs) and 169 associated Targets.

To track progress towards these Goals and Targets, the global indicator framework must capture the multi-faceted and ambitious aspirations for the continued development of nations and societies. Effective reporting of progress toward these indicators will require the use of multiple types of data, both what we have in hand - traditional national accounts, household surveys and routine administrative data –and new sources of data outside national statistical systems, notably Earth observation (EO) and geospatial information (GI), and 'Big Data' in general.

The integration of all these data can produce a quantum leap in how we monitor and track development and advance the well-being of our societies. Since Earth observation and geospatial information are often continuous in their spatial and temporal resolutions, their use in SDG monitoring can prove essential in capturing the sustainability of developments underpinning the SDG framework. Earth observation and geospatial information, which include satellite, airborne, land- and marine-based data, as well as model outputs, will expand monitoring capabilities at local, national, regional and global levels, and across sectors.

Earth observation and geospatial information can significantly reduce the costs of monitoring the aspirations reflected in the goals and targets, and make SDG monitoring and reporting viable within the limited resources available to governments. Beyond the SDG framework, these same data can provide developing countries and regions with increased capacity to acquire, analyse and utilise information for a broad range of policy-making purposes.

The Japan Space Exploration Agency (JAXA) is actively promoting use of satellite-based Earth observations for SDGs through the Comittee on Earth Observation Satellites (CEOS) and the intergovernmental Group on Earth Observations (GEO) in cooperation with national statistical office and related ministries and agencies, and UN and other interantional organizations. Current status of JAXA activities for exploring the applications of satellilte based Earth observations to SDGs and their prospects will be presented.

Keywords: SDGs, Sustainable Developmetn Goals, indictor framework, Earth observation

GPM SLH latent heating retrievals with a study on extratropical precipitation systems

*Yukari Takayabu[1], Chie Yokoyama[1], Atsushi Hamada[1], Shoichi Shige[2], Munehisa Yamamoto[2], Moeka Yamaji[3], Takuji Kubota[3], Yasutaka Ikuta[4]

1. Atmosphere and Ocean Research Institute, the University of Tokyo, 2. Kyoto University, 3. Japan Aerospace Exploration Agency, 4. Japan Meteorological Agency

Diabatic heating associated with convection plays essential roles in energy budget in the global atmosphere, driving large-scale circulation, and intensifying various kinds of storms. Dual-frequency Precipitation Radar on board the Global Precipitation Measurement core satellite (GPM DPR) has expanded our ability to consider such convective latent heating in the extratropical regions, in addition to tropical regions where we have estimated the latent heating with the Tropical Rainfall Measuring Mission Precipitation Radar (TRMM PR) observations (TRMM Spectral Latent Heating algorithm; Shige et al. 2004, 2007, etc.). In order to construct an algorithm to retrieve the convective latent heating in the extratropics, we examined the relationship between the precipitation and latent heating in extratropical environments, utilizing GPM DPR data with the aid of cloud-resolving numerical model simulations, contrasting it with tropical precipitation.

For the SLH retrieval algorithm in the tropics, we simulated the TOGA-COARE precipitation with the Goddard Cumulus Ensemble Model, from which we made three spectral look-up tables (LUT) of latent heating profiles for convective, shallow stratiform rain, and deep stratiform rain. Utilizing TRMM PR rain profiles as well as GPM Ku-band Precipitation Radar (KuPR) rain profiles with these tables, we retrieved the latent heating associated with precipitation in tropical and subtropical regions.

Extratropical precipitation consists of systems very different from the tropics. The most dominant system there is the extratropical cyclone and associated frontal systems. The largest difference may reside in the stratiform precipitation. While deep stratiform precipitation is associated with deep convection in the tropics almost without exception, in the extratropics, large-scale ascent associated with frontal systems can result in deep stratiform precipitation from the large-scale condensation. The deep stratiform cloud base in the tropics is, therefore, almost fixed at the freezing level, but it does not necessarily correspond to the freezing level in the extratropics.

As a strategy to obtain adequate LUTs for extratropical systems, with a collaboration of the JMA numerical weather forecast group, we collected forecast run outputs for extratropical systems with the JMA Local Forecast Model (LFM). With these data, we analyzed the simulated precipitation and latent heating for extratropical systems, to produce LUTs for GPM KuPR.

To this end, we had to overcome several hurdles: (1) To obtain consistent LFM and KuPR precipitation flux, (2) to attain consistent convective/stratiform separation, (3) to obtain adequate cloud-base and freezing level relationships, (4) to detect cloud base adequately from the GPM KuPR, and (5) to handle multi-layer precipitations. After solving these problems, we obtained convective precipitation tables looked up with precipitation top heights, and stratiform precipitation tables looked up with cloud-base precipitation intensities. Results from applications of GPM KuPR data to these latent heating LUTs also will be discussed.

# GOES-16 Advanced Baseline Imager (ABI) On-Orbit Performance

*Paul Griffith[1], Sheldon Drobot[1], John Van Naarden[1]

1. Harris Corporation

The GOES-16 Advanced Baseline Imager (ABI) is the first of the United States' next-generation geostationary imagers for weather and environmental monitoring. The design and capabilities are the same as Himawari-8 and -9, but with some differences in the spectral bands. With three times the spectral bands, four times the resolution, and five times the image collection rate, the GOES-16 ABI will significantly improve the quality and frequency of existing data products and provide many new weather and environmental products. It is currently undergoing post launch testing and is scheduled to become operational in November 2017.

The ABI post-launch test campaign takes place from January to June 2017. These tests verify compliance with requirements as well as thoroughly characterize the performance of the instrument, including long-term performance trending. This presentation provides measured, quantitative performance results showing the very high quality of ABI's imagery, including SNR and NEdT, MTF, line-of-sight stability, navigation and registration, and calibration stability. Although the post-launch testing will not be complete, all of these critical performance aspects will have been measured and trended. Understanding the quality of this imagery is the first step in assessing the quality of the many ABI-based L2+ data products.

Keywords: weather, satellite, geostationary, ABI, GOES
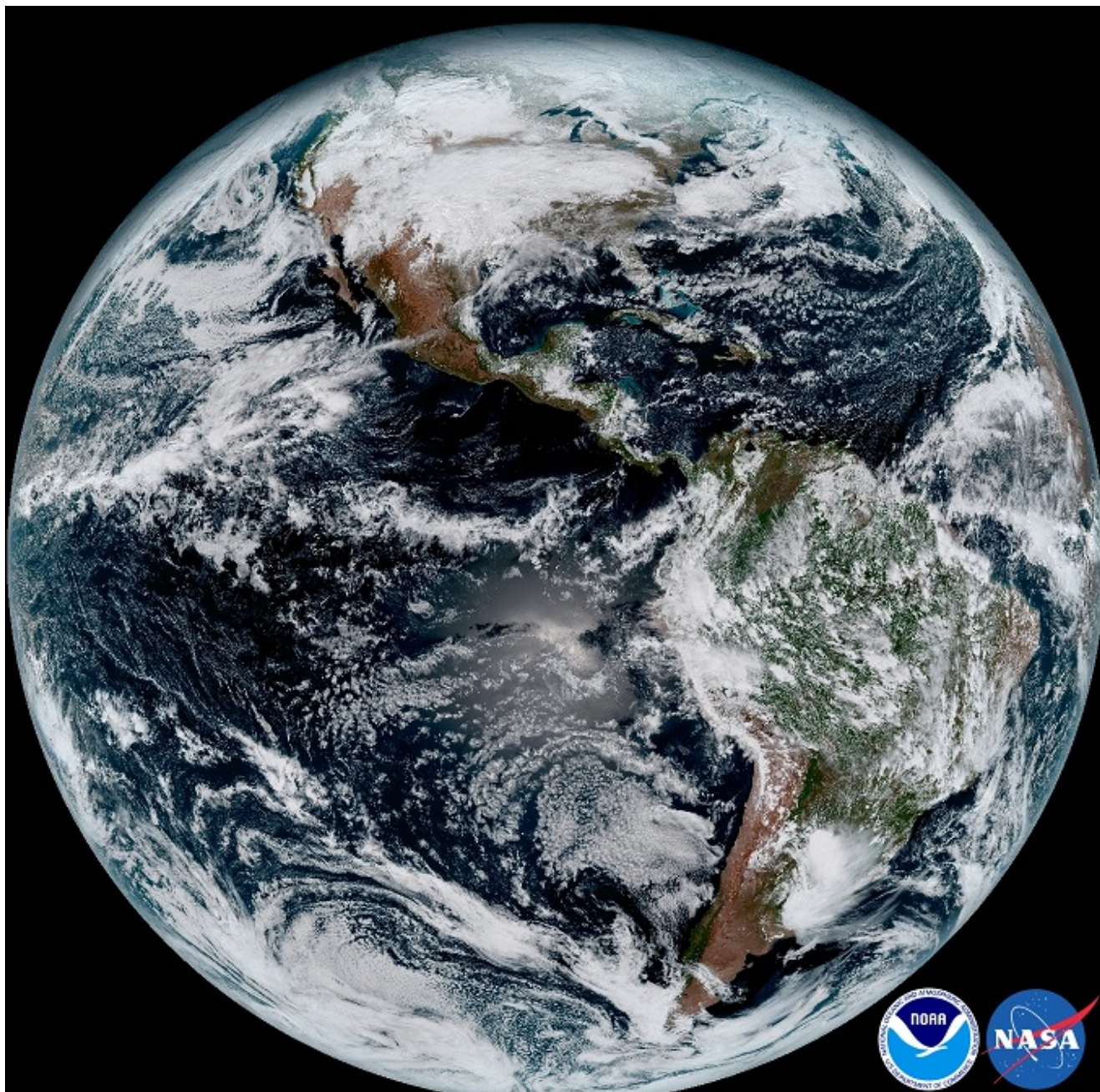
Five years Global Water Cycle Observation by the Global Change Observation Mission - Water (GCOM-W)

Taikan Oki[1,2], *Misako Kachi[2,3], Takashi Maeda[2], Hiroyuki Tsutsui[2], Nodoka Ono[2], Marehito Kasahara[3], Masaaki Mokuno[3]

1. Institute of Industrial Science, The University of Tokyo, 2. Earth Observation Research Center, Japan Aerospace Exploration Agency, 3. GCOM Project Team, Japan Aerospace Exploration Agency

The Global Change Observation Mission (GCOM) is consists of two medium sized satellites to provide comprehensive information of the Essential Climate Variables (ECV) of atmosphere, ocean, land, cryosphere, and ecosystem. The GCOM-W (Water) or "SHIZUKU" satellite that is carrying the Advanced Microwave Scanning Radiometer 2 (AMSR2), which was launched from JAXA Tanegashima Space Center on May 18, 2012 (JST); and GCOM-C (Climate) satellite that will carry the Second Generation Global Imager (SGLI) and is scheduled to be launched in Japanese Fiscal Year of 2017.

AMSR2 on board the GCOM-W satellite is multi-frequency, total-power microwave radiometer system with dual polarization channels for all frequency bands, and a successor of JAXA's Advanced Microwave Scanning Radiometer for EOS (AMSR-E) on the NASA's Aqua satellite, which was launched in May 2002, and completed its operation in December 2015. Basic concept of AMSR2 is almost identical to that of AMSR-E. AMSR2 standard products, including brightness temperature and eight geophysical parameters that related to water cycle, have been introduced to many operational and science applications quickly. AMSR2 standard products are available from the GCOM-W1 Data Providing Service (https://gcom-w1.jaxa.jp/). The latest version of AMSR2 products is Ver. 2.0 (as of February 2017) that was released in March 2015, and JAXA is planning to release new Version 3 standard products for several geophysical parameters, including sea surface temperature and sea surface wind speed, which do not satisfy required standard accuracies in Ver.2, in March 2017. With release of Ver.3 standard products, all AMSR2 standard products satisfy required standard accuracy and achieve mission success criteria of the GCOM-W mission.

AMSR2 products are used in various operational and research fields, including weather forecast, typhoon analysis, global rainfall map, ocean monitoring, fisheries, sea ice extent monitoring and maritime navigation in polar regions. At the meeting, we will highlight major topics of achievements done by the GCOM-W mission in five years.

Since designed mission life of the GCOM-W satellite is five years and will be achieve in May 2017, we have started discussion of possible follow-on mission with various user communities as well as expansion of application of AMSR2 and follow-on data in new fields.

Keywords: satellite remote sensing, water cycle, microwave radiometer

Development of CloudSat/CALIPSO- and EarthCARE-algorithms for studies of cloud macroscale- and microphysical properties

*Hajime Okamoto[1], Kaori Sato[1], Shuichiro Katagiri[1]

1. Kyushu University

This work improved on cloud mask, cloud particle type and cloud microphysics algorithms that can be applied to CloudSat-CALIPSO and EarthCARE satellites. We first revised the cloud mask algorithm designed for CALIPSO lidar developed by Hagihara et al., to increase the detectability of cloud bottom regions in CALIPSO lidar observations. Algorithm for cloud particle type (cloud phase and orientation of ice particles) developed by Yoshida et al., is also refined. Introducing the new function, cloud particle phase near cloud bottom is better characterized by the revised algorithm. Retrieval algorithm for ice cloud microphysics is also carried out to extend the one developed by Sato and Okamoto with modified look up tables for ice particles. That for water cloud microphysics was newly implemented.

The refinements were achieved by using the new type of ground-based lidar, Multiple-Field of View Multiple Scattering Polarization lidar (MFMSPL) with cloud radar. MFMSPL was designed to measure enhanced backscattering and depolarization ratio comparable to space-borne lidar. The system consists of five sets of parallel and perpendicular channels with different zenith angles. We first evaluated our former cloud mask scheme. It was applied to the data obtained by the MFMSPL and it was found that the cloud mask scheme underestimated cloud top portions. New cloud mask scheme showed improvement in the detectability of cloud top portions. Co-located 95GHz cloud radar and MFMSPL with the new cloud mask scheme showed good agreement at the cloud top altitude. The cloud mask scheme also has a function to identify fully attenuated pixels where lidar and cloud radar signals are totally attenuated.

Our former cloud particle type algorithm was evaluated by the observed attenuated backscattering coefficient and depolarization ratio by off-beam channels of MFMSPL. Extinction-depolarization ratio diagram is created based on the observed data. The analyses of MFMSPL show that large depolarization ratio with small attenuation can be caused by water clouds. The features have not observed in the CALIPSO lidar data since our former cloud mask scheme did not detect cloud bottom portions in the analysis of CALIPSO lidar data and such features are found in the regions newly detected by the improved cloud mask algorithm. The new feature is implemented in the refined cloud particle type algorithm to better discriminate ice and water where lidar signals are largely attenuated and depolarization ratio increased.

We report the results of global analyses of cloud fraction, ice/water fraction and ice/water microphysics by using CloudSat and CALIPSO. We also discuss possible extension of the algorithms for cloud profiling radar (CPR) and high spectral resolution lidar (ATLID) on EarthCARE.

Keywords: cloud, radar, lidar

Global water cloud microphysics from active sensor synergy toward the EarthCARE mission

*Kaori Sato[1], Hajime Okamoto[1], Shuichiro Katagiri[1]

1. RIAM, Kyushu Univ.

Retrieval of global water cloud microphysics from space-borne lidar and cloud radar is on focus. Issues exists in how quantitatively multiple scattering effects from vertically inhomogeneous cloud layers are estimated for microphysical inversion, and in the reliability of low-level cloud detection in this connection. In our previous studies, A prototype of the microphysics retrieval algorithm combining the lidar attenuated backscattering coefficient, depolarization ratio and Cloud radar observables were developed for particle sizing and cloud particle-drizzle mass ratio estimates. There, the lidar returns from inhomogeneous clouds were simulated by combining look-up-tables of the parallel and perpendicular components for homogeneous profiles according to their contribution to the total path to reflect inhomogeneity effects. In this study, improvements were made in that area to replace the former approach by a numerically effective and flexible physical model that traces the exact Monte Carlo simulations, and to further meet the technical requirements for global retrieval. Preliminary results from CloudSat/CALIPSO data analysis showed the effectiveness of the synergy algorithm in tracking the vertical variation of cloud properties. Global analysis of water cloud microphysics will be further carried out together with a refined low-level cloud detection scheme.

Keywords: space-borne lidar/radar, cloud

Ice crystal number concentration estimates from lidar-radar satellite remote sensing

*Odran Sourdeval[1], Edward Gryspeerdt[2], Julien Delanoë[3], Johannes mülmenstädt[1], Christine Nam[1], Friederike Hemmer[4], Johannes Quaas[1]

1. University of Leipzig, Leipzig, Germany, 2. Imperial College London, London, UK, 3. LATMOS/UVSQ/IPSL/CNRS, Guyancourt, France, 4. Laboratoire d'Optique Atmosphérique, Université Lille1, Villeneuve d'Ascq, France

Recent assessments from the climate research community clearly highlight the emergency to reach a better understanding of aerosol-cloud interactions in order to improve current radiative forcing estimates. Satellite observations are ideal to fulfill this task due to their high temporal and spatial coverage, but their operational products are not always suited to answer these questions. Indeed, while the number concentration of cloud droplets (CDNC) and ice crystals (ICNC) are often considered as some of the most important parameters to quantify aerosol-cloud interactions, they are not yet optimally retrieved from satellite remote sensing. Despite recent efforts to estimate the CDNC, there exists to date no space-borne operational product of the ICNC.

As a first step to fill this gap, this study presents results from a preliminary product of the ICNC obtained from combined CALIPSO/CloudSat observations. The operational liDAR-raDAR (DARDAR) product is used as a basis for these estimations. Climatologies corresponding to the overall A-Train period have been analyzed and show an overall agreement with theoretical expectations. Furthermore, the accuracy of these ICNC retrievals has been rigorously estimated through comparisons with in situ measurements from recent airborne campaigns. Good agreements are found for ice clouds colder than about -40˚C, where homogeneous nucleation processes dominate. Limitations have nevertheless been observed due to misrepresentations of the amount of small ice particules (i.e., sizes smaller than 100 microns) in existing parameterizations of the particle size distribution. Subsequently, preliminary applications of this novel dataset to evaluated global climate model predictions and observe aerosol-cloud interactions have been made and will be presented.

Keywords: ice clouds, satellite, retrievals, model evaluation, aerosol-cloud interactions

Ice particle morphology and microphysical properties of transparent cirrus clouds inferred from CALIOP–IIR measurements

*Masanori Saito[1], Hironobu Iwabuchi[1], Ping Yang[2], Guanglin Tang[2], Michael D King[3], Miho Sekiguchi[4]

1. Tohoku University, 2. Texas A&M University, 3. University of Colorado, 4. Tokyo University of Marine Science and Technology

Microphysical properties and ice particle morphology of cirrus clouds are important for estimating the radiative forcing associated with these clouds. Many satellite measurements allow us to estimate the cloud optical thickness (COT) and cloud-particle effective radius (CER) of cirrus clouds over the globe via multiple retrieval methods such as the bi-spectral method using visible and near-infrared cloud reflectivities, the split-window method using thermal infrared brightness temperatures and the unconstrained method using lidar signals. However, comparisons among these retrievals exhibit discrepancies in some cases due to particular error sources for each method. In addition, methods to infer ice particle morphology of clouds from satellite measurements are quite limited. To tackle these current problems, we develop an optimal estimation based algorithm to infer cirrus COT, CER, plate fraction including horizontally oriented plates (HOPs) and the degree of surface roughness from the Cloud Aerosol Lidar with Orthogonal Polarization (CALIOP) and the Infrared Imaging Radiometer (IIR) on the Cloud Aerosol Lidar and Infrared Pathfinder Satellite Observation (CALIPSO) platform. A simple but realistic ice particle model is used, and the bulk optical properties are computed using state-of-the-art light-scattering computational capabilities. A rigorous estimation of the uncertainties related to the surface properties, atmospheric gases and cloud heterogeneity is performed. A one-month global analysis for April 2007 with a focus on HOPs shows that the HOP fraction has significant temperature dependence and therefore latitudinal variation. Ice particles containing many HOPs have small lidar ratio due to strong backscattering. The lidar ratio of cirrus clouds has a negative correlation with the temperature where the cloud temperature is warmer than −40℃, for which the median HOP fraction is larger than 0.01%.

Keywords: Cloud properties, Satellite remote sensing, Oriented ice crystals

The retrieval of ice-cloud properties from Himawari-8/AHI

*Husi Letu[1,2], Takashi M. Nagao[3], Takashi Y. Nakajima[2], Hiroshi Ishimoto[4], Huazhe Shang[1], Liangfu Chen[1]

1. Institute of Remote Sensing and Digital Earth, Chinese Academy of Sciences (CAS), 2. Research and Information Center (TRIC), Tokai University, 3. Earth Observation Research Center (EORC), JAXA, 4. Meteorological Research Institute

Himawari-8 satellite was successfully launched in October 2014, which carry a multi-spectral sensor of Advanced Himawari Imager (AHI). The AHI cloud products were developed by employing the cloud algorithm of the GCOM-C satellite program, which included cloud mask, thermodynamic phase, cloud optical, microphysical properties and cloud types. Some of the cloud products (e.g. cloud optical thickness and cloud types) are archived in JAXA homepage (http://www.eorc.jaxa.jp/ptree/). Cloud products from remote sensing instrument is applicable in climate change study, numerical weather prediction, meteorological disaster, as well as atmospheric study. In this study, ice cloud optical and microphysical properties are simulated from RSTAR radiative transfer code by using various ice particle scattering models. Scattering property of the Voronoi ice particle scattering model is investigated for developing the AHI ice cloud products. Furthermore, optical and microphysical properties of the ice clouds are retrieved from Himawari-8/AHI satellite measurements. Finally, retrieval results from Himawari-8/AHI are compared to MODIS-C6 cloud property products for validation of the AHI cloud products.

Keywords: Ice cloud, Remote sensing, Ice particle scattering property

Validation of Himawari-8 and MODIS observed water cloud microphysical and optical properties using ground-based observation data

*Pradeep Khatri[1], Tadahiro Hayasaka[1], Hironobu Iwabuchi[1], Hitoshi Irie[2], Kazuaki Kawamoto[3]

1. Graduate School of Science,Tohoku University, 2. Center for Environmental Remote Sensing, Chiba University, 3. Graduate School of Fisheries and Environmental Sciences, Nagasaki University

Along with the development of remote sensing technology, cloud remote sensing from the space has become a very powerful tool to gather information related to clouds, including cloud optical and microphysical characteristics, by covering sufficiently large areas. Those data are being implemented to cope/understand several issues related to climate change and hydrological cycle phenomena. Due to such broad implications, quality check of such space-observed cloud properties takes a very high priority. Such quality check can be fundamentally done by using ground-truth data; however, retrieval of cloud properties from ground-based observation data itself is a challenging task, which has also limited validation of cloud products made from observations by several sensors onboard several satellites. Taking this difficulty into account, we developed a cloud retrieval method by implementing spectral transmittances of near-infrared wavelengths observed by zenith-looking sky radiometer of SKYNET (http://atmos2.cr.chiba-u.jp). The retrieval accuracy has been quantified and cloud products from sky radiometer along with surface-observed global flux data of four SKYNET sites (Chiba, Fukuejima, Hedomisaki, and Miyakojima) of nearly one year period have been used to validate water cloud properties observed by the Himawari-8, a Japanese geostationary satellite, and the MODIS sensor onboard the TERRA and AQUA earth observation satellites. The temporal variation of cloud optical thickness (COD) from three independent instruments (Sky radiometer, MODIS, Himawari-8) is consistent, though they differ in magnitude. Generally speaking, COD from MODIS is found to be underestimated followed by Himawari 8 and sky radiometer. The underestimation of COD from satellite observations could be further justified by CODs estimated from the global flux data by assuming the fixed value of effective radius (Re). On the other hand, Re from MODIS is found to be overestimated followed by Himawari-8 and sky radiometer. The overestimation of Re from satellite observations is consistent with prior studies. Data of long-term observation are being analyzed to quantify the error ranges of MODIS and Himawari-8 observed cloud properties (particularly COD) with respect to surface-based sky radiometer and global flux data. Similar analyses to validate ice cloud properties observed from satellites will be performed in the near future.

Keywords: Cloud, Satellite, SKYNET, Sky radiometer

Accomplishments from 3-years of Global Precipitation Measurement (GPM) Data: NASA's Perspective

*Gail Skofronick Jackson[1], George J Huffman[1]

1. NASA Goddard Space Flight Center

Precipitation is a key source of freshwater; therefore, the observation of global patterns of rain and snow and their intensity is important for science, society, and understanding our planet in a changing climate. In 2014, NASA and the Japan Aerospace Exploration Agency (JAXA) launched the Global Precipitation Measurement (GPM) Core Observatory (GPM-CO) spacecraft. The GPM-CO carries the most advanced precipitation sensors currently in space including a Dual-frequency Precipitation Radar (DPR) provided by JAXA measuring the three-dimensional structures of precipitation and a well-calibrated, multi-frequency passive microwave imaging radiometer (GPM Microwave Imager –GMI) providing wide-swath precipitation data. The GPM-CO was designed to measure rain rates from 0.2-110.0 mm h^{-1} and to detect moderate to intense snow events. The GPM-CO is a key part of the GPM mission, which is defined to encompass multi-satellite unified precipitation estimates. The GPM-CO serves as a reference for unifying data from a constellation of about 10 (in 2016) partner satellites (see Fig. 1) to provide next-generation, merged precipitation estimates globally and with high temporal (0.5 to 3.0 hours) and spatial (5 to 15 km) resolutions. Through improved measurements of rain and snow, precipitation data from GPM provides new information such as: details of precipitation structure and intensity; observations of hurricanes and typhoons as they transition from the tropics to mid-latitudes; data to advance near-real-time hazard assessment for floods, landslides and droughts; inputs to improve weather and climate models; and insights into agricultural productivity, famine, and public health. Since launch, GPM teams have calibrated satellite instruments, refined precipitation retrieval algorithms, expanded science investigations, and processed and disseminated precipitation data for a range of applications.

The GPM-CO spacecraft is an advanced successor to the Tropical Rainfall Measuring Mission (TRMM), with additional channels on both the DPR and GMI with capabilities to sense light rain and falling snow (Hou et al., 2014, Hou et al., 2008). The GPM-CO was launched at 18:37 UTC 27 February 2014 and operates in a non-sun-synchronous orbit with an inclination angle of 65˚ (Fig. 2). The prime mission lifetime (instrument design life) is 2 months for checkout and 3 years for operations, but operations could last 15-24 years according to fuel projections in November 2016 (see Appendix E for fuel charts) assuming the instruments/spacecraft systems (e.g., batteries) do not fail and fuel requirements do not increase. The inclined orbit allows the GPM-CO to sample precipitation across all hours of the day from the Tropics to the Arctic and Antarctic Circles. GPM expands TRMM's reach not only in terms of global coverage, but also through more sophisticated satellite instrumentation, systematic inter-calibration of datasets from other microwave radiometers, refined merged precipitation data sets, reduced latency for delivering data products, simplified data access, expanded global ground-validation efforts, and integrated user applications. Because of the application focus of GPM, the public release of precipitation products is required in NRT (1-5 hours after the observations are downlinked to the ground stations).

Accomplishments of the Prime Mission lifetime (March 2014-May 2017) can be categorized into four topics: Instrument calibration, Improvements in the Retrieval Algorithm, Progress toward the Scientific Objectives of the GPM mission, and Meeting the GPM Level 1 Mission Requirements. These accomplishments and future activities will be presented.

Keywords: Earth, Satellite, Precipitation, GPM

Three-year results of the Global Precipitation Measurement (GPM) mission in Japan

*Riko Oki[1], Takuji Kubota[1], Kinji Furukawa[1], Yuki Kaneko[1], Moeka Yamaji[1], Toshio Iguchi[2], Yukari Takayabu[3]

1. Japan Aerospace Exploration Agency, 2. NICT, 3. The University of Tokyo

The Global Precipitation Measurement (GPM) mission is an international collaboration to achieve highly accurate and highly frequent global precipitation observations. The GPM mission consists of the GPM Core Observatory jointly developed by U.S. and Japan and Constellation Satellites that carry microwave radiometers and provided by the GPM partner agencies. The GPM Core Observatory, launched on February 2014, carries the Dual-frequency Precipitation Radar (DPR) by the Japan Aerospace Exploration Agency (JAXA) and the National Institute of Information and Communications Technology (NICT). JAXA develops the DPR Level 1 algorithm, and the NASA-JAXA Joint Algorithm Team develops the DPR Level 2 and DPR-GMI combined Level2 algorithms. The Japan Meteorological Agency (JMA) started the DPR assimilation in the meso-scale Numerical Weather Prediction (NWP) system on March 24 2016. This was regarded as the world 's first "operational" assimilation of spaceborne radar data in the NWP system of meteorological agencies.

JAXA also develops the Global Satellite Mapping of Precipitation (GSMaP), as national product to distribute hourly and 0.1-degree horizontal resolution rainfall map. The GSMaP near-real-time version (GSMaP_NRT) product is available 4-hour after observation through the "JAXA Global Rainfall Watch" web site (http://sharaku.eorc.jaxa.jp/GSMaP) since 2008. The GSMaP_NRT product gives higher priority to data latency than accuracy, and has been used by various users for various purposes, such as rainfall monitoring, flood alert and warning, drought monitoring, crop yield forecast, and agricultural insurance. There is, however, a requirement for shortening of data latency time from GSMaP users. To reduce data latency, JAXA has developed the GSMaP real-time version (GSMaP_NOW) product for observation area of the geostationary satellite Himawari-8 operated by the Japan Meteorological Agency (JMA). GSMaP_NOW product was released to public in November 2, 2015 through the "JAXA Real-time Rainfall Watch" web site (http://sharaku.eorc.jaxa.jp/GSMaP_NOW/).

All GPM standard products and the GPM-GSMaP product have been released to the public since September 2014 as Version 03. The GPM products can be downloaded via the internet through the JAXA G-Portal (https://www.gportal.jaxa.jp). The DPR, the GMI, and the DPR-GMI combined algorithms will be updated in April 2017 and the latent heating product will be released in June 2017 as Version 04. New calibration factors will be applied for both Ku and Ka-band radars. As its results, values of Z factor will increase, but estimated value of rain intensity does not necessarily increase. Also calibration factors of TRMM/PR will be re-examined to have consistency between DPR/Ku. Furthermore, the GPM-GSMaP algorithms were updated and the GPM-GSMaP Version 04 products have been provided since Jan. 2017.

Keywords: GPM, Satellite Remote Sensing, Precipitation

DSD database for the GPM/DPR precipitation retrieval algorithm

*Shinta Seto[1], Natsuki Iwama[1], Kenta Miyazaki[2], Toshio Iguchi[3]

1. Graduate School of Engineering, Nagasaki University, 2. School of Engineering, Nagasaki University, 3. National Institute of Information and Communications Technology

Rain Drop Size Distribution (DSD) has been and is being measured with disdrometers at many stations in the world. Parameterization of DSD is necessary for retrieving rain rates (R) from radar measurements. The relation between radar reflectivity factor (Z) and R (Z-R relation) is an example of DSD parameterization. In the precipitation retrieval algorithm of the Dual-frequency Precipitation Radar (DPR) of the Global Precipitation Measurement (GPM) mission core satellite, the relation between the mass-weighted mean drop size (D_m) and R (R-D_m relation) is used. As both R and D_m are independent of radar frequency, R-D_m relation is useful in the dual-frequency algorithm and it may be extended for other radar measurements. The standard R-D_m relation in the DPR algorithm was derived from Z-R relation which Kozu et al. (2009) proposed based on precipitation measurements in Tropics. It may not be appropriate and need to be modified for mid- and high-latitude precipitation within the DPR coverage.

In the DPR algorithm, at each pixel, R-D_m relation is modified by the Surface Reference Technique (SRT), while the SRT does not work well for light precipitation. However, dual-frequency measurements make it possible to adjust R-D_m relation for light precipitation.

The figure shows estimates of R and D_m for over-land convective precipitation cases by single-frequency (SF) algorithm (Fig. a) and dual-frequency (DF) algorithm (Fig. b) in the version-4 DPR algorithm. For weak precipitation, SF algorithm mostly follows the standard R-D_m relation, but DF algorithm gives larger D_m estimates.

Based on DF estimates, optical R-D_m relations are calculated for seasons and regions. They are summarized as DSD database. The new R-D_m relations are used for SF algorithm in the version-5 DPR algorithm (Fig. c). As a result, SF and DF algorithms give closer D_m for weak precipitation. As the next step, the DSD database needs to be validated and improved with ground-based measurements.

Keywords: GPM, DPR, drop size distribution
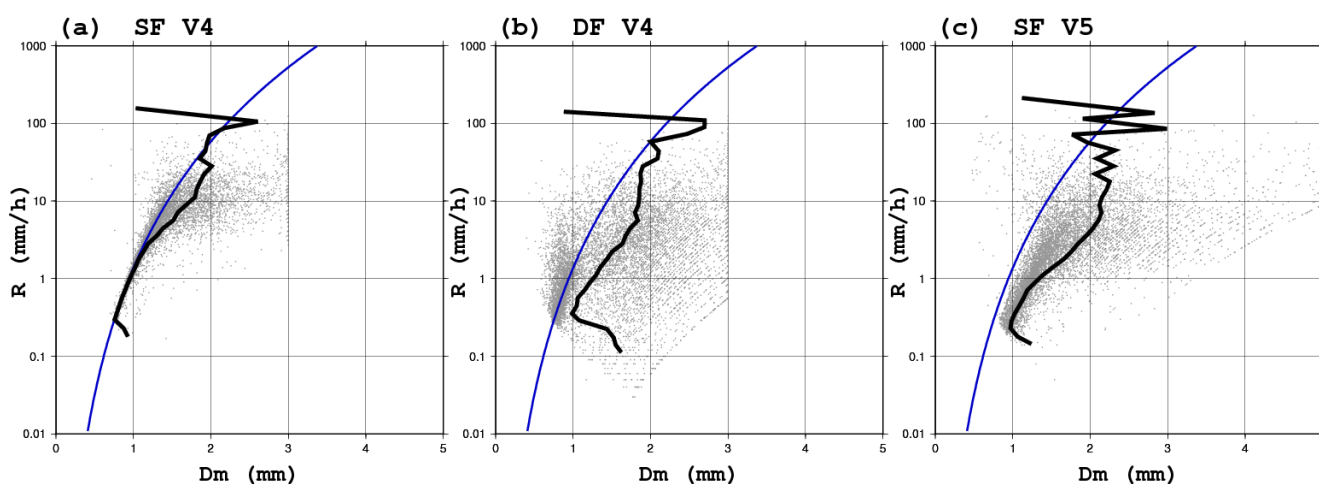
Improving Physically Based Retrievals of Rain and Snow over Land Surfaces for the GPM Constellation

*Sarah Ringerud[1], Gail Skofronick Jackson[1], Christa Peters-Lidard[1]

1. NASA Goddard Space Flight Center

The joint NASA/JAXA Global Precipitation Measurement Mission (GPM) offers an unprecedented opportunity for development of highly accurate global rain and snowfall observation. Utilizing the GPM core satellite as a transfer standard, physically based Bayesian retrievals are applied consistently across a constellation of passive microwave radiometers for increased observations in both time and space. The use of a physically based retrieval scheme also allows for connection of the retrieval to models and physical processes, integrating them in valuable ways for the study of the processes themselves and more general Earth system science.

While the utility of the Bayesian retrieval has been well demonstrated over ocean surfaces, the relatively high surface emissivity in the microwave region over land and snow-covered areas makes the distinguishing of the precipitation signal more difficult. As the emission signals at lower frequency are extremely difficult to differentiate from the emissive land background, the scattering signal is the primary indicator of precipitation in this case, and the higher frequency channels more heavily weighted. Two crucial areas for such retrievals are therefore identified for improvement: accurate representation of scattering radiative transfer in the high frequency channels of the retrieval *a priori* database, and accurate identification of the surface characteristics for database indexing.

Early versions of GPM constellation retrievals model ice particles in the *a priori* database as spheres. Comparisons of radiative transfer results suggest that spherical particles do not correctly reproduce observed scattering in the high frequency channels, and that non-spherical particle radiative transfer is required for multispectral agreement. In order for the Bayesian retrieval scheme to choose the correct precipitation profiles, the radiative transfer must be accurate. For this work the full retrieval database is recomputed using non-spherical particles and the retrieval results compared.

Land surfaces in the current GPM constellation retrievals are classified statically, using a climatology of self-similar retrieved emissivities. Such a classification does not account for dynamic surface changes such as dramatic soil moisture shifts due to rainfall that have a large dielectric effect. For this work alternative classification using dynamically assessed land surface characteristics of soil moisture and vegetation is tested within the retrieval algorithm and compared to retrievals using the static classification.

Sensitivity to both the scattering radiative transfer and the dynamic definition of surface type will be demonstrated in the context of the full retrieval algorithm and a path forward suggested for improved performance.

Keywords: precipitation, remote sensing, passive microwave retrieval

Recent progress in Global Satellite Mapping of Precipitation (GSMaP) product

*Takuji Kubota[1], Kazumasa Aonashi[2], Tomoo Ushio[3], Shoichi Shige[4], Yukari Takayabu[5], Yoriko Arai[6], Tomoko Tashima[6], Misako Kachi[1], Riko Oki[1]

1. Earth Observation Research Center, Japan Aerospace Exploration Agency, 2. Meteorological Research Institute, Japan Meteorological Agency, 3. Osaka University, 4. Kyoto University, 5. University of Tokyo, 6. Remote Sensing Technology Center of Japan

The Global Precipitation Measurement (GPM) mission is an international collaboration to achieve highly accurate and highly frequent global precipitation observations. As one of Japanese GPM products, Global Satellite Mapping of Precipitation (GSMaP) product has been provided by Japan Aerospace Exploration Agency (JAXA) to distribute hourly global precipitation map with 0.1x0.1 deg. lat/lon grid. The GSMaP products are composed of "standard product", "near-real-time product", "real-time product", and "reanalysis product". The standard products are processed 3 days after observation, and the near-real-time products are processed 4 hours after observation. In addition, the real-time version, GSMaP_NOW has been provided by the JAXA over the geostationary satellite "Himawari-8" region since Nov. 2015.
Recently, the GSMaP algorithms were majorly updated on September 2014 and January 2017.
Major improvements on September 2014 are following. 1) Improvements in microwave imager algorithm based on AMSR2 precipitation standard algorithm, including new land algorithm, new coast detection scheme; 2) Development of orographic rainfall correction method for warm rainfall in coastal areas; 3) Update of database, including rainfall detection over land and land surface emission database; 4) Development of microwave sounder algorithm over the land; and 5) Development of gauge-calibrated GSMaP algorithm. In addition to those improvements in the algorithms, a number of input passive microwave imagers and/or sounders was increased using the GMI and the GPM Constellation Satellites. Major improvements on January 2017 are following. 1) Improvement of the GSMaP algorithm using GPM/DPR observations as its database; 2) Implementation of a snowfall estimation method in the GMI & SSMIS data, based upon Liu and Seto (2013) and Sims and Liu (2015) and a screening method using NOAA multisensor snow/ice cover maps in all sensors; 3) Improvement of the gauge-correction method in both near-real-time and standard products; 4) Improvement of the orographic rain correction method; 5) Improvement of a weak rain detection method over the ocean by considering cloud liquid water.
The current paper describes overviews of the GSMaP products and recent progress of the GSMaP product.

Keywords: Precipitation, Satellite, Remote Sensing

Development of the GEO-KOMPSAT-2A AMI rainfall rate algorithm

*Damwon So[1], Dong-Bin Shin[1]

1. Dept. of Atmospheric Sciences, Yonsei Univ.

A rainfall rate algorithm has been developed for the Advanced Meteorological Imager (AMI) onboard the GEO-KOMPSAT-2A (GK-2A), the second Korea's geostationary satellite, scheduled to be launched in early 2018. The AMI rainfall rate algorithm uses the a-priori information including the microwave rainfall data from the low-earth orbiting satellites and infrared (IR) brightness temperatures from geostationary satellites. The algorithm may better perform with a variety of a-priori information describing all possible precipitating systems. In addition, separation of physically different precipitating systems likely to improve the accuracy of retrieval process. However, it has been well known that such the separation can be hardly achieved based on the measurements of cloud top temperatures. This algorithm tries to utilize the radiative characteristics observed differently for different wavelengths in IR spectral regions. The characteristics include the different emissivity as a function of wavelength and cloud thickness. Using the brightness temperature differences (BTDs) between IR channels the algorithm discriminates three types of precipitating clouds: shallow, not-shallow-tall and not-shallow-taller types. The separation of three types of precipitating clouds may help the accuracy of rainfall estimates for each type of clouds. In addition to the separation of cloud types in the databases, the algorithm also uses databases classified by latitudinal bands. The bands are separated with four latitudinal zones. The separation of database based on latitudes may have an effect of distinguishing the cloud types that can occur regionally. The a-priori databases are thus classified with 12 different categories. Once the a-priori databases are constructed, the algorithm inverts the AMI IR brightness temperatures to the surface rainfall rate based on a Bayesian approach. The Bayesian approach has advantages on using multi-channel brightness temperatures simultaneously and utilizing the probability of rainfall reserved in the a-priori databases. As a proxy for the AMI this algorithm first tests the Advanced Himawari Imager (AHI) data. Retrieval results and the status and plan of the algorithm development will be introduced.

Keywords: GK-2A, AMI, Rainfall rate algorithm

Studies on future spaceborne precipitation measuring mission

*Nobuhiro Takahashi[1], Kinji Furukawa[2], Yusuke Muraki[2], Daisuke Joudoi[2], Riko Oki[2]

1. Institute for Space-Earth Environmental Research, Nagoya University, 2. Japan Aerospace Exploration Agency

Dual frequency precipitation radar (DPR) onboard the core satellite of the Global Precipitation Measurement (GPM) has been demonstrated its feasibilies for three years. In the scientific viewpoint, GPM/DPR is contributing to provide precipitation structures globally including snowfall over 90 % of global coverage, almost 20 years of accumulation of accurate global rainfall (mainly tropics to sub-tropics) since the observation by the precipitation radar (PR) onboard the Tropical Rainfall Measuring Mission (TRMM) satellite, and hourly global precipitation map (such as GSMaP) by combining not only the sensors onboard the GPM/core satellite but also the satellites that equip microwave radiometer. The societal importance of the space based precipitation observation has changed since the launch of the TRMM. The TRMM mission is rather a process-study mission to reveal the three dimensional heating profiles of the precipitation systems especially for the tropical rainfall systems. Success of the TRMM in terms of the accurate precipitation measurement and long-term observation period, provision of the accurate precipitation map was added for the TRMM's roll. Global precipitation maps such as GSMaP which is one of major purposes of GPM provide hourly 0.1 degree in latitude/longitude data and utilized for the flood forecasting/warning system, agricultural applications and so on. On the technological aspect, the success of the GPM/DPR has shown maturities of its technology such active phased array system using slotted waveguide antenna, solid state power amplifier and so on. In addition, recent studies on the pulse compression technology and the TRMM end of mission experiment (Takahashi et al., 2016) indicate the further advances of the spaceborne precipitation radar are possible with current technology.

Based on achievements of TRMM and GPM, science targets of the future precipitation mission have been discussed among the GPM science community.

One of the science targets is cloud-precipitation processes. Since the cloud and precipitation interaction is important process of the precipitation formation. Both the cloud and precipitation observation is also very helpful to evaluate the cloud physical processes of the numerical climate models. The societal contribution target will be to improve GSMaP both on the accuracy and data latency.

For these purposes, three types of missions are considered: 1)small radar constellation satellites to upgrade the GSMaP product by replace the passive microwave estimation by radar estimation (radar constellation), 2) development of the DPR type radar with better sensitivity and the wider swath observation based on the advances on the solid state power amplifier and the wide swath operation of the TRMM EOM experiment (DPR2), and 3) radar observation of precipitation from geostationary satellite (GPR).

Feasibility studies for these missions have started on the key elements such as precipitation estimation accuracy for radar constellation satellite, feasibility study on the pulse compression technology for wide swath operation of DPR2, and feasibility of the large antenna design and the clutter mitigation for GPR. Time scale of these missions are different; DPR2 is almost ready to move the development phase, the development of small radar for the radar constellation needs the feasibility of small antenna system through bread board model (BBM) development, and several fundamental technologies such as deployable large size antenna are needed to demonstrate in orbit for GPR.

Keywords: precipitation observation mission, radar

Evaluation of potential benefits of outer-loop iteration for all-sky microwave imager radiance assimilation at JMA's global NWP system

*Masahiro Kazumori[1], Takashi Kadowaki[1]

1. Japan Meteorological Agency

In numerical weather prediction (NWP), assimilation of cloud and precipitation affected radiance is essential to obtain accurate initial fields in cloudy areas. Cloud and precipitation phenomena have non-linear behaviors in their formation and dissipation. To consider such non-linearity in an incremental four dimensional variational (4D-Var) data assimilation, outer-loop iteration is necessary for re-computation of departures from the observations and updates of trajectory in minimizations of the 4D-Var.

The impacts on tropical cyclone prediction from all-sky microwave imager radiance assimilation using JMA's global NWP system were presented at the last conference in 2016. The system used in the experiment had no use of the outer-loop iteration as same configuration of JMA's operational global NWP system. In this research, we investigated impacts of the outer-loop iteration for the all-sky microwave imager radiance assimilation. Three data assimilation experiments were performed to compare with a control run whose configuration was same to current operational JMA's global NWP system: all-sky microwave imager radiance assimilation experiment (EXP1), outer-loop introduced experiment (EXP2), and their combined experiment (EXP3). The EXP1 results indicate the positive impacts on tropical cyclone's track and intensity predictions from the all-sky assimilation by improving analyses in the cloudy areas which are meteorologically sensitive and where no useful information is obtained from current clear-sky assimilation. The EXP2 results demonstrated large positive impacts from the outer-loop introduction on analysis and forecast accuracy of geopotential height, tropospheric temperature, humidity, and wind fields.

The comparison between the EXP1 and EXP3 which can indicate the impact of the outer-loop iteration on the all-sky radiance assimilation reveals that the introduction of outer-loop iteration increased assimilated existing humidity sensitive observations (e.g., microwave humidity sounder radiances) and improved the analysis accuracy. However, the gains from the all-sky assimilation for the forecast skill were similar. One possible reason of this result is a discrepancy of cloud and precipitation representation between inner and outer model in the 4D-Var system. To get further benefits from the outer-loop iteration in the all-sky assimilation, a consistent cloud and precipitation representation between the models would be necessary.

The details of the latest experiment results and the issues are discussed in the conference.

Assimilation of Satellite Soil Moisture Contents and Clear-sky Radiance in Operational Local NWP System at JMA

*Yasutaka Ikuta[1]

1. Japan Meteorological Agency

The Japan Meteorological Agency (JMA) operates the Local NWP system constructed with the high-resolution Local Forecast Model (LFM) and Local Analysis. LFM and Local Analysis are run hourly and various types of the latest observation are assimilated.

JMA started to assimilate the satellite observation of clear-sky radiance (CSR) and soil moisture content (SMC) in the Local NWP system in January 2017. The assimilated radiance data are CSR observation from Himwari-8 AHI, GPM GMI, GCOM-W AMSR2, Metop-A/B AMUS-A/MHS and DMSP SSMIS. And the assimilated SMCs are those of L2-products from GCOM-W AMSR2 and Metop-A/B ASCAT. These SMC are assimilated after variable transformation using cumulative distribution function (CDF) matching method. The CDF matching method fits the probability density function (PDF) of observation to the PDF of model variables. This pre-conditioning by CDF matching helps to minimize the cost function because the innovation of SMC becomes Gaussian after the CDF matching. However, it is known that the observation bias of satellite fluctuate over time. To remove adaptively such bias of the secular changes, the variational bias correction method is adopted in the Local Analysis. As a result, both the CSR and SMC can be assimilated as unbiased observation and the forecast accuracy of atmosphere and surface is improved. The impact of these satellite data assimilation will be presented.

Application of aggregated non-spherical ice-phase particle modeling to assimilation of GPM radiance observations in meso-scale NWP

*Sara Q Zhang[1], Philippe Chambon [2], William Olson [1]

1. NASA Goddard Space Flight Center, Greenbelt, MD, USA, 2. Meteo France, Toulouse, France

Variations in the distributions of ice-phase cloud and precipitation particles are important indicators of dynamical and physical processes in atmosphere, but at the same time, the representation of these particle types and the underlying processes in numerical weather prediction model forecasts are often subject to substantial errors. Since ice-phase cloud/precipitation can have a significant impact on upwelling microwave radiances at the higher microwave frequencies (85 –183 GHz) through the scattering process, assimilation of satellite microwave observations into model-supported analyses has the potential to correct for model errors. Crucial to the assimilation of these observations are forward radiative models that can be used to simulate higher-frequency microwave radiances based on forecast earth/atmosphere states. In this work we present the development and improvements in forward modeling of using aggregated non-spherical ice-phase particles to calculate microwave single-scattering properties with particle size distribution descriptions based of field campaign studies. Experiments are carried out using NASA Unified Weather Research Forecast ensemble data assimilation system. All-sky radiance observations from NASA/JAXA Global Precipitation Measurement (GPM) mission Microwave Imager (GMI) are assimilated into high-resolution model forecasts. The impact of both the input data and the forward modeling on first-guess radiance departures and analyzed/forecast fields are investigated in case studies of mid-latitude snowstorm and warm season convective storm overland.

Keywords: satellite observations, precipitation, data assimilation

Model Parameter Estimation Using Ensemble Data Assimilation: A Case with the Nonhydrostatic Icosahedral Atmospheric Model NICAM and the Global Satellite Mapping of Precipitation Data (GSMaP)

*Shunji Kotsuki[1], Koji Terasaki[1], Hisashi Yashiro[1], Hirofumi Tomita[1], Masaki Satoh[2], Takemasa Miyoshi[1]

1. RIKEN Advanced Institute for Computational Science, 2. Atmosphere and Ocean Research Institute, The University of Tokyo

This study aims to improve precipitation forecasts from numerical weather prediction (NWP) models through effective use of satellite-derived precipitation data. Kotsuki et al. (2017, JGR-A) successfully improved the precipitation forecasts by assimilating the Japan Aerospace eXploration Agency (JAXA)'s Global Satellite Mapping of Precipitation (GSMaP) data into the Nonhydrostatic Icosahedral Atmospheric Model (NICAM) at 112-km horizontal resolution. Kotsuki et al. mitigated the non-Gaussianity of the precipitation variables by the Gaussian transform method for observed and forecasted precipitation using the previous 30-day precipitation data.

This study extends the previous study by Kotsuki et al. and explores an online estimation of model parameters using ensemble data assimilation. We choose two globally-uniform parameters, one is the cloud-to-rain auto-conversion parameter of the Berry's scheme for large scale condensation and the other is the relative humidity threshold of the Arakawa-Schubert cumulus parameterization scheme. We perform the online-estimation of the two model parameters with an ensemble transform Kalman filter by assimilating the GSMaP precipitation data. The estimated parameters improve the analyzed and forecasted mixing ratio in the lower troposphere. Therefore, the parameter estimation would be a useful technique to improve the NWP models and their forecasts. This presentation will include the most recent progress up to the time of the meeting.

Keywords: Data Assimilation, GSMaP precipitation, NICAM, LETKF, Parameter Estimation

Assimilation of cloudy infrared radiances of the geostationary Himawari-8 imager

*NAOTAKA UEKIYO[1], KOZO OKAMOTO[1], DAISAKU UESAWA[2], RYO YOSHIDA[2], YUSUKE IOKA[2]

1. Meteorological Research Institute/JMA, 2. Meteorological Satellite Center/JMA

We introduce the current status of experiment of assimilating cloud-affected infrared observation from a geostationary satellite, Hiamawari-8, into JMA global numerical weather prediction model. Infrared observation data from geostationary satellites such as Himawari-8 are contributing to improving analysis and forecast accuracy in numerical weather prediction.
However, cloud-affected observation data are rarely used in the practical assimilation system due to the nonlinearity physical process in clouds, complex and non-Gaussian statistics and so on. Assimilation of cloud-affected observation data is crucial for improving the accuracy of analyses and forecasts in numerical weather prediction(NWP).
The radiance data to be assimilated were created by averaging pixels from the original radiances (ASR, or All Sky Radiance), which was developped at Meteorological Satellite Center (MSC) in 2016. In this study, we assimilated infrared radiances by assuming a single layer cloud ("simple cloud"), in which cloud effect in radiative transfer is calculated simply by using the cloud-top pressure and an effective fraction of cloud.
The results of the experiments so far showed that even with this simple treatment, appropriately selected data offer valuable information not available from cloud-free observations.

Keywords: satellite observation, Himawari-8, data assimilation, numerical weather prediction, cloudy
            observation

Eight Years of GOSAT Operation in Space and New Science from GOSAT-2

*Tsuneo Matsunaga[1], Tatsuya Yokota[1], Masakatsu Nakajima[2], Gen Inoue[3], Ryoichi Imasu[4]

1. Center for Global Environmental Research and Satellite Observation Center, National Institute for Environmental Studies, 2. Japan Aerospace Exploration Agency, 3. University of Tsukuba, 4. The University of Tokyo

Greenhouse Gases Observing Satellite (GOSAT) and its successor, GOSAT-2, are Japanese earth observing satellites for greenhouse gases (GHG) measurements from space. Both satellite projects are joint efforts among Ministry of the Environment (MOE), Japan Aerospace Exploration Agency (JAXA), and National Institute for Environmental Studies (NIES).

GOSAT was launched in January 2009 and has been operated for more than eight years. It has a Fourier transform spectrometer (FTS) for the measurements of columnar abundances of carbon dioxide (CO_2) and methane and a UV-VIS-NIR-SWIR imager (CAI) for cloud and aerosol detection. Its data are being used in various scientific researches related to climate change and atmospheric pollution monitoring such as monitoring of whole-atmosphere monthly mean carbon dioxide concentration, evaluation of inventories for anthropogenic emissions of CO_2 and methane, and PM2.5 mapping in asian urban regions.

GOSAT-2 will be launched in FY2018. GOSAT-2 instruments (FTS-2 and CAI-2) will be modified or improved based on the experiences of GOSAT instruments. FTS-2 will have the extended spectral coverage for carbon monoxide measurement and the intelligent pointing capability to avoid cloud contamination. CAI-2 will have multiple UV bands for more precise land aerosol monitoring and the forward/backward viewing capability to avoid sun glint over oceans. GOSAT-2's spacecraft, instruments, and ground data processing systems are currently being manufactured.

In this presentation, several scientific achievements based on GOSAT's eight-year GHG data and new science expected from GOSAT-2 will highlighted.

GOSAT-2 science plan and recent progress in sensor development for CO_2 monitoring over mega-cities from space

*Ryoichi Imasu[1], Tsuneo Matsunaga[2], Tatsuya Yokota[2]

1. Atmosphere and Ocean Research Institute, The University of Tokyo, 2. National Institute for Environmental Studies

Greenhouse gases Observing Satellite (GOSAT) was launched on January 23, 2009, and it has provided worldwide scientists with high quality observational data for more than 7 years. The primary purpose of the mission is to reduce the posterior error in inversion analysis of CO_2 source/sink strengths by about 50% in some sub-continental scales (several thousand kilometers square). As have already showed by previous studies (e.g., Takagi et al., 2011), the original purpose has been accomplished on a project basis. Based on these successful results, its successor, GOSAT-2 has been designed and developed to be launched in FY2018. At the same time, the science team of the project started discussion on its scientific objectives to be summarized as "Science Plan". Most important obligation for the project to the scientific community is the continuity of the observational data connecting from GOSAT project with the same or, hopefully better quality. The improvement of signal-to-noise ratio (SNR) of TANSO-2 Fourier transform spectrometer/GOSAT-2 ensures the continuity, and furthermore observable regions could be expanded toward higher latitudes and the region size of inversion analyses is expected to be able to be smaller. Its scientific objectives can be classified into four categories for CO_2; 1) fusion of bottom-up and top-down approaches in budget analyses, 2)up grading of prediction performances of land-ecosystem models and coupling to the inversion models, 3)improvement of detectability of hotspots, and 4)contribution to REDD+ by providing the relevant community with desired data. As for CH_4, 1)detection of changes in emissions from wetlands attributing to global warming, 2)watching the gas leaks from pipelines, 3)monitoring the emission from agricultural sources, and 4)investigations on the long-term trend of increasing rate of atmospheric concentration. Recently, satellite sensors of which instantaneous field of view (IFOV) is narrow enough to resolve emission sources in mega-cities have been developed (e.g., CLAIRE/GHGsat). However, their calibration accuracies are not necessarily better than preexisting sensors. One possible way to apply these sensors to monitor small emissions with useful accuracy is combining the sensors with well calibrated sensors such as GOSAT-2 on radiance or higher product level basis. In this point of view, GOSAT-2 sensors are expected to keep the highest performance of accuracy.

Keywords: GOSAT-2, science plan, mega-city

GHG Observations of GOSAT/TANSO-FTS TIR band: data quality and scientific findings

*Naoko Saitoh[1], Ryosuke Nonogaki[1], Shingo Kosaka[1], Akinori Yamada[1], Ryoichi Imasu[2], Kei Shiomi[3], Akihiko Kuze[3], Yosuke Niwa[4], Toshinobu Machida[5], Yousuke Sawa[4], Kazuhiro Tsuboi[4], Hidekazu Matsueda[4], Yu Someya[2]

1. Center for Environmental Remote Sensing, Chiba University, 2. Atmosphere and Ocean Research Institute, The University of Tokyo, 3. Japan Aerospace Exploration Agency, 4. Meteorological Research Institute, 5. National Institute for Environmental Studies

The Greenhouse Gases Observing Satellite (GOSAT) has continued its observations of greenhouse gases (GHG) such as CO_2 and CH_4 for almost 8 years since its launch on 23 January 2009. The Thermal and Near Infrared Sensor for Carbon Observation (TANSO)–Fourier Transform Spectrometer (FTS) on board GOSAT consists of three bands in the short-wave infrared (SWIR) region and one band in the thermal infrared (TIR) region (Kuze et al., 2009). From the TANSO-FTS TIR spectra, CO_2 and CH_4 concentrations are retrieved in several atmospheric layers; the latest TIR Level 2 (L2) retrieval product is version 1 (V1) (Saitoh et al., 2016).

We have evaluated the bias in the CO_2 concentrations of the TIR V1 L2 CO_2 product of the GOSAT/TANSO-FTS based on comparisons with data from the Continuous CO_2 Measuring Equipment (CME) in the Comprehensive Observation Network for TRace gases by AIrLiner (CONTRAIL) project (Machida et al., 2008) in the upper troposphere and lower stratosphere (UTLS), the middle troposphere (MT), and the lower troposphere (LT) for the 3 years from 2010 to 2012. Here, we used the CME data obtained during the level flights over a wide area and the ascent and descent flights over several airports for the comparisons in the UTLS region and the ML and LT regions, respectively. Furthermore, we examined the validity of the bias assessment over limited areas over the airports by comparing TIR CO_2 data globally with CO_2 data simulated by the Nonhydrostatic ICosahedral Atmospheric Model (NICAM)-based transport model (TM) (Niwa et al., 2011). The comparison results in the UTLS region showed that TIR CO_2 data had larger negative biases in spring and summer (>2 ppm) than in fall and winter in the northern low and middle latitudes (Saitoh et al. 2016), and the biases became larger over time. This is because TIR UT CO_2 data were constrained by the a priori data whose growth rates were ~1.4 ppm/yr from 2010 to 2012, which was less than the growth rates based on CME data (~2.1 ppm/yr). However, TIR UT CO_2 data displayed seasonal variations that were more similar to the CME data than to the a priori data. The amplitudes of the seasonal variations were comparable, except at the northern middle latitudes. In the ML and LT regions (736−287 hPa), TIR CO_2 data had negative biases against CME CO_2 data in the latitude range between 40°S and 60°N in all seasons. They had the largest negative biases in retrieval layers 5−6 (541−398 hPa), which mainly came from the retrieval at the CO_2 10-μm absorption band (930−990 cm^{-1}). Comparisons between NICAM-TM CO_2 data and bias-corrected TIR CO$_2$ data to which the bias-correction values evaluated over the airports were applied showed that the median values of their differences were closer to zero, which demonstrates the validity of the bias-correction values; we conclude that the bias-correction values defined the comparisons in limited areas over airports can be applicable to TIR CO_2 data in areas other than the airport locations.

We compared TIR V1 L2 CH_4 data with data obtained over Minamitorishima by a C-130H cargo aircraft (Tuboi et al., 2013; Niwa et al., 2014) and with data obtained in a wide latitude range during the HIAPER Pole-to-Pole Observation (HIPPO) aircraft campaign (Wofsy et al., 2011). The comparison results showed that TIR CH_4 data agreed with the aircraft CH_4 data to within ~1% in the MT and LT regions in the northern middle latitudes in spring, fall and winter, although they had negative biases of 1.2−1.5% in the MT region

in summer. TIR CH_4 data in the MT regions agreed with HIPPO CH_4 data to within 1% in low latitudes and in the southern middle latitudes, which is consistent with the results of Zou et al. (2016) and Olsen et al. (2017).

Philippines TCCON Installation: Towards Quantifying Atmospheric Carbon in Southeast Asia

*Isamu Morino[1], Voltaire A. Velazco[2,4], Akihiro Hori[1], Osamu Uchino[1], Tetsu Sakai[3], Toshiharu Izumi[3], Tomohiro Nagai[3], David W. T. Griffith[2]

1. National Institute of Environmental Studies, 2. University of Wollongong, 3. Meteorological Research Institute, 4. Oscar M. Lopez Center for Climate Change Adaptation and Disaster Risk Management Foundation, Inc.

The Total Carbon Column Observing Network (TCCON) is dedicated to the precise measurements of greenhouse gases such as CO_2 and CH_4. TCCON measurements have been and are currently used extensively and globally for satellite validation, for comparison with atmospheric chemistry models and to study atmosphere-biosphere exchanges of carbon. With the global effort to cap greenhouse gas emissions, TCCON has taken on a vital role in validating satellite-based greenhouse gas data from past, current and future missions like Japanese GOSAT and GOSAT-2, NASA's OCO-2 and OCO-3, Chinese TanSat, and others. The lack of reliable validation data for the satellite-based greenhouse gas observing missions in the tropical regions is a common limitation in global carbon-cycle modeling studies that have a tropical component. The international CO_2 modeling community has specified a requirement for "expansion of the CO_2 observation network within the tropics" to reduce uncertainties in regional estimates of CO_2 sources and sinks using atmospheric transport models. A TCCON site in the western tropical Pacific is a logical next step in obtaining additional knowledge that would greatly contribute to the understanding of the Earth's atmosphere and better constraining a major tropical region experiencing tremendous economic and population growth.
An assessment for possible sites in the Philippines where TCCON FTS should be installed were performed and we decided to install it at Burgos site (the substation of Energy Development Corporation Burgos Wind Farm Project), Ilocos Norte, Philippines (18.5326° N, 120.6496° E). We characterized a performance of the newly constructed TCCON instrument intended for deployment to the Philippines and made initial measurements at the NIES compound in Japan. After development in Japan, we deployed TCCON FTS at Burgos site in Dec. 2016 and conducted installation/set up of instruments until Mar. 2017. Then we could get the first light measurements in Philippines. Here, we will present the whole picture of the Philippines TCCON project.

Keywords: Carbon-cycle, Greenhouse Gas, Total Carbon Column Observing Network, Satellite Validation

Natural and anthropogenic contributions to long-term variations of SO$_2$, NO$_2$, CO and aerosol over East China

*Hanqing Kang[1,2,3,4], Bin Zhu[1,2,3,4]

1. Key Laboratory for Aerosol-Cloud-Precipitation of China Meteorological Administration, Nanjing University of Information Science & Technology, Nanjing, China, 2. Collaborative Innovation Center on Forecast and Evaluation of Meteorological Disasters, Nanjing University of Information Science & Technology, Nanjing, China, 3. Key Laboratory of Meteorological Disaster, Ministry of Education (KLME), Nanjing University of Information Science & Technology, Nanjing, China, 4. Joint International Research Laboratory of Climate and Environment Change (ILCEC), Nanjing University of Information Science & Technology, Nanjing, China

East China has been experiencing significant air pollution during the past decades. Long-term variations of air pollutants over East China are affected by increasing energy consumption, government pollution regulation, new technologies, economic conditions, human activities and a number of natural factors such as global warming, long-term variations in precipitation, monsoon strength etc. Quantifying the impacts of natural oscillations and anthropogenic activities on the long-term variations of air pollutants is critical for guiding emission control measures. In this study, satellite-retrieved and MOZART-4-simulated SO$_2$, NO$_2$, CO and total column aerosol mass concentration (AMC) data are used to investigate the impacts of natural factors and human activities on long-term variations of these air pollutants over East China. The Kolmogorov–Zurbenko (KZ) filter is used to extract long-term trends from both observed and simulated air pollutant data. Results show that SO$_2$ concentrations decreased from 2007 to 2014, with natural and anthropogenic factors contributing 37.4% and 62.6% to this decrease, respectively. NO$_2$ concentrations increased significantly during 2000–2014; anthropogenic activities contribute 79.5% to this variation, while natural factors only account for 20.5%. CO concentrations decreased slowly from 2003 to 2009, with contributions of natural and anthropogenic factors of 19% and 81%, respectively. Since 2006, AMC decreased slightly, with natural factors accounting for 43% of the total variation, while human activities account for 57%.
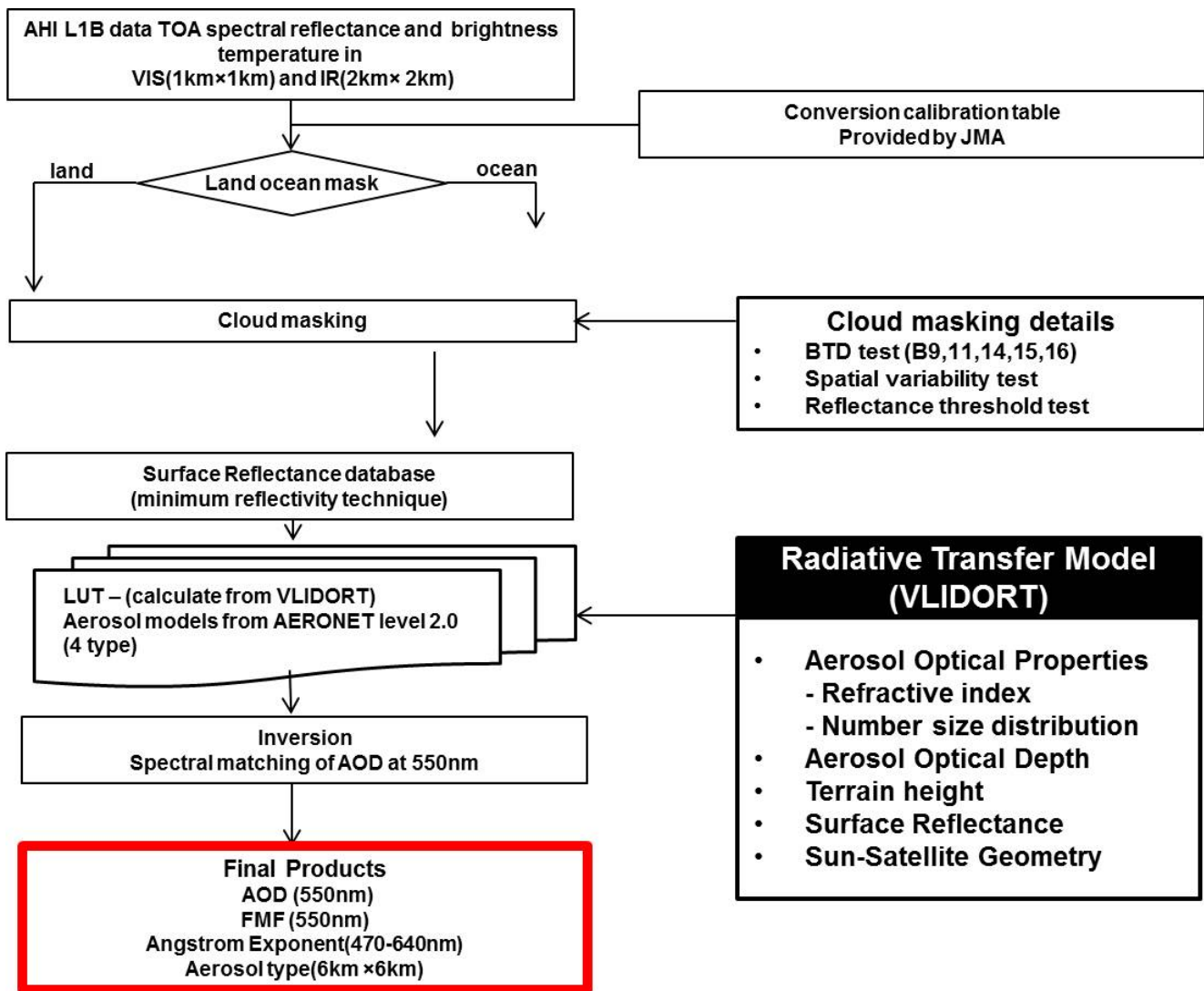
Keywords: satellite observation, MOZART-4 model, contribution

Description of Advanced Himawari Imager (AHI) Yonsei aerosol retrieval algorithm Version 1

*Hyunkwang Lim[1], Jhoon Kim[1], Myungje Choi[1], Sujung Go[1], P W Chan[2], Yasuko Kasai[3]

1. Yonsei University, 2. Hong Kong Observatory, 3. National Institute of Information and Communications Technology

Japan Meteorological Agency (JMA) successfully launched the next-generation geostationary satellite called Himawari-8 in 7 October 2014 and started a formal operation in 7 July 2015. The Advanced Himawari Imager (AHI) sensor having 16 channels (from 0.47 to 13.3 μm) is the next-generation geostationary satellite that observes the full disk every 10 minutes. This study attempts to retrieve the aerosol optical properties (AOPs) based on the spectral matching method, with using three visible and one near infrared channels (470, 510, 640, 860nm). This method requires the preparation of look-up table (LUT) approach based on the radiative transfer modeling. Cloud detection is one of the most important processes for guaranteed quality of AOPs. Since the AHI has several infrared channels, which are very advantageous for cloud detection, clouds can be removed by using brightness temperature difference (BTD) and spatial variability test. The Yonsei Aerosol Retrieval (YAER) algorithm is basically utilized on a dark surface, therefore a bright surface (e.g., desert) should be removed first. Then we consider the characteristics of the reflectance of land and ocean surface using three visible channels. The known surface reflectivity problem in high latitude area can be solved in this algorithm by selecting appropriate channels through improving tests. Based on validation results with the sun-photometer measurement in AErosol Robotic NETwork (AERONET), we confirm that the quality of Aerosol Optical Depth (AOD) from the YAER algorithm is comparable to the product from the Japan Aerospace Exploration Agency (JAXA) retrieval algorithm. Our future update includes a consideration of surface reflectance at ocean BRDF and non-spherical aerosols. This will improve the quality of YAER algorithm more, particularly retrieval for the dust particle over the bright desert surface in East Asia.

AHI L1B data TOA spectral reflectance and brightness temperature in
VIS(1km×1km) and IR(2km× 2km)

Conversion calibration table
Provided by JMA

land — Land ocean mask — ocean

Cloud masking

Cloud masking details
- BTD test (B9,11,14,15,16)
- Spatial variability test
- Reflectance threshold test

Surface Reflectance database
(minimum reflectivity technique)

LUT – (calculate from VLIDORT)
Aerosol models from AERONET level 2.0
(4 type)

**Radiative Transfer Model
(VLIDORT)**

- **Aerosol Optical Properties**
  - Refractive index
  - Number size distribution
- **Aerosol Optical Depth**
- **Terrain height**
- **Surface Reflectance**
- **Sun-Satellite Geometry**

Inversion
Spectral matching of AOD at 550nm

Final Products
AOD (550nm)
FMF (550nm)
Angstrom Exponent(470-640nm)
Aerosol type(6km ×6km)

Development and acceleration of aerosol remote sensing algorithm and its application to GOSAT/TANSO-CAI data

*Makiko Hashimoto[1], Hideaki Takenaka[1], Akiko Higurashi[2], Teruyuki Nakajima[1]

1. Japan Aerospace Explortion Agency, 2. National Institute for Environmental Studies

Aerosol in the atmosphere is an important atmospheric constituent for determining the earth's radiation budget, especially perturbation by the human activity, so the accurate aerosol retrievals from satellite is useful. We have developed a satellite remote sensing algorithm to retrieve the aerosol optical properties using multi-wavelength and multi-pixel information of satellite imagers (MWPM). The method simultaneously derives aerosol optical properties, such as aerosol optical thickness (AOT) and single scattering albedo (SSA), by using spatial difference of surface reflectance. Thus, the method is useful for aerosol retrieval over spatially heterogeneous surface like an urban region. We apply an optimal method and spatial smoothness constraint for aerosol properties, and directly combining with the radiation transfer calculation/model (RTM), Rstar (Nakajima and Tanaka, 1986, 1988), numerically solved by each iteration step of the non-linear inverse problem, without using Look Up Table. The merit of direct use of RTM is that: more accurate multiple scattering calculations in more realistic atmospheric conditions are available; it is easy to change retrieval parameters or wavelengths. Therefore, more accurate and flexible retrievals can be expected. However, it has also weak point that it takes a large computation time compared to that with LUT method. To accelerate the calculation time, we replace the RTM with an accelerated RTM solver learned by neural network-based method (Takenaka et al., 2011), EXAM, using Rater code. We apply MWPM with EXAM to GOSAT/TANSO-CAI (CAI) imager data. CAI has four bands, 380, 674, 870 and 1600 nm, and observes in 500 meters resolution for band1, band2 and band3, and 1 km for band4. The retrieved parameters are fine and coarse mode AOTs, SSA and surface reflectance at each wavelength by combining a minimum reflectance method and Fukuda et al. (2013). As a result, the calculation time was shortened from about 10 second to 0.01 second per pixel. And also, the similar retrieval results are obtained compared with MWPM with RTM over Beijing region.

Keywords: Aerosol, Remote sensing

Spectrally Dependent Calibration Requirement for CLARREO IR Instrument

*Xu Liu[1]

1. NASA Langley Research Center, Hampton, VA 23681, USA

The infrared (IR) spectrometer of the Climate Absolute Radiance and Reflectivity Observatory (CLARREO) will measure the Top of Atmospheric (TOA) thermal radiance spectra from 200 to 2000 cm^{-1}. It is designed to detect trends of atmospheric temperature, moisture, cloud, and surface properties even in the presence of measurement gaps. Wielicki et al [1] have studied the CLARREO measurement requirements for achieving climate change absolute accuracy in orbit. The goal of this study is to further quantify the spectrally dependent calibration requirement for CLARREO IR instrument. Spectral fingerprinting method is used to evaluate how the calibration error affects our ability to detect the changes that are smaller than the natural variability of temperature and moisture. The temperature, humidity, and surface skin temperature variability and the associated correlation time are derived using Modern Era Retrospective-Analysis for Research and Applications (MERRA) and European Center for Medium-Range Weather Forecasts (ECMWF) reanalysis data. The results are further validated using the climate model simulation results. To detect an accurate trend for a geophysical parameter, the observation system has to be able to separate the natural variability from the climate changes. Therefore, even for a perfect observation system, one has to make long enough observations to minimize the contribution from the natural variability. With the derived natural variability and correlation time as the reference, the calibration requirement for the IR instrument can be deduced based on a spectral fingerprinting method.

Keywords: Climate trend detection, remote sensing, satellite instrument intercalibration

Evaluation of ozone profile and tropospheric ozone retrievals from GEMS and OMI spectra

*Jae Hwan Kim[1]

1. Department of Atmospheric Science

South Korea is planning to launch the GEMS (Geostationary Environment Monitoring Spectrometer) instrument into the GeoKOMPSAT (Geostationary Korea Multi-Purpose SATellite) platform in 2018 to monitor tropospheric air pollutants on an hourly basis over East Asia. GEMS will measure backscattered UV radiances covering the 300–500 nm wavelength range with a spectral resolution of 0.6 nm. The main objective of this study is to evaluate ozone profiles and stratospheric column ozone amounts retrieved from simulated GEMS measurements. Ozone Monitoring Instrument (OMI) Level 1B radiances, which have the spectral range 270–500 nm at spectral resolution of 0.42–0.63 nm, are used to simulate the GEMS radiances. An optimal
estimation-based ozone profile algorithm is used to retrieve ozone profiles from simulated GEMS radiances. Firstly, we compare the retrieval characteristics (including averaging kernels, degrees of freedom for signal, and retrieval error) derived from the 270–330 nm (OMI) and 300–330 nm (GEMS) wavelength ranges. This comparison shows that the effect of not using measurements below 300 nm on retrieval characteristics in the troposphere is insignificant. However, the stratospheric ozone information in terms of DFS decreases greatly from OMI to GEMS, by a factor of 2. The number of the independent pieces of information available from GEMS measurements is estimated to 3 on average in the stratosphere, with associated retrieval errors of 1% in stratospheric column ozone. The difference between OMI and GEMS retrieval characteristics is apparent
for retrieving ozone layers above 20 km, with a reduction in the sensitivity and an increase in the retrieval errors for GEMS. We further investigate whether GEMS can resolve the stratospheric ozone variation observed from high vertical resolution EOS MLS. The differences in stratospheric ozone profiles between GEMS and MLS are comparable to those between OMI and MLS below 3 hPa (40 km), except with slightly larger biases and larger standard deviations by up to 5 %. At pressure altitudes above 3 hPa, GEMS retrievals show strong influence of a priori and large differences with MLS, which, however, can be sufficiently improved by using better a priori information. The GEMS-MLS differences show negative biases of less than 4% for stratospheric column ozone, with standard deviations of 1–3 %, while OMI retrievals show similar agreements with MLS except for 1% smaller biases at middle and high latitudes. Based on the comparisons, we conclude that GEMS will measure tropospheric ozone and stratospheric ozone columns with accuracy comparable to that of OMI and ozone profiles with slightly worse performance than that of OMI below 3 hPa.

Keywords: Geostationary enviomental satellite, ozone, profile

High-performance clear-sky temperature and humidity information from geostationary imagers and their applications to short-term weather forecasting

*Su Jeong Lee[1], Myoung-Hwan Ahn[1], Sung-Rae Chung[2]

1. Department of Atmospheric Sciences and Engineering, Ewha Womans University, South Korea, 2. National Meteorological Satellite Center, South Korea

As more and more high-performance imagers are flying in geostationary orbits, there has been growing interest in how to utilize the imager-derived products and how accurate those products are. Although researchers and forecasters have already been provided with very accurate data from the numerical weather prediction (NWP) model or hyperspectral sounders onboard the polar orbiters, both type of data are provided in lower temporal and spatial resolution when compared to that from high-resolution imagers such as the Advance Himawari Imager (AHI) on board Himawari-8 that is operating on orbit or the Advanced Meteorological Imager (AMI) on board Korea's 2nd generation geostationary satellite, Geo-KOMPSAT-2A, scheduled to launch in 2018. Furthermore, NWP model accuracy decreases in the presence of clouds or in data sparse areas. This study focuses on this aspect, emphasizing the advantage of using high-resolution products, particularly moisture related products, retrieved from the AHI through a couple of case studies and suggests the potential benefits of using those products for short-range severe weather forecasting. Product accuracy is evaluated using radiosonde measurements, NWP model analysis, and Radio-Occultation measurements. Presentation will cover a brief introduction to the retrieval algorithm, which is based on an optimal estimation method with the unified model forecast as the first guess to produce clear-sky vertical profiles of temperature and moisture and other atmospheric parameters such as total precipitable water and instability indices. Algorithm characteristics and validation results will be also presented during the conference.

Keywords: high-performance geostationary imager, temperature and humidity profile retrieval algorithm, short-term weather forecasting, optimal estimation

Constructing an ocean data assimilation product using satellite sea surface temperature

*Tsutomu Hihara[1], Yasumasa Miyazawa[1], Toru Miyama[1], Misako Kachi[2], Hiroshi Murakami[2], Yukio Kurihara[2], Noboka Ono[2], Hidenori AIKI[3]

1. Japan Agency for Marine-Earth Science and Technology, 2. Japan Aerospace Exploration Agency, 3. Nagoya University

The Japan Aerospace Exploration Agency (JAXA) operates the several earth observation satellites, and provides satellite sea surface temperature (SST) data. Satellite capability to detect SST data is advancing in recent year. For example, the Himawari-8 which was launched in 2014 is able to detect SST around Japan every 10 minutes. However, a satellite SST dataset includes some missing depending on the type of satellite and sensor, and doesn't provide the vertical ocean data. In this study, we construct a temporally and spatially uniform ocean dataset, using a data assimilation method which combines the satellite SST data and the ocean model data.

Our target area is south of Japan where the Kuroshio flows. The data assimilation technique and ocean model which we use are the Local Ensemble Transform Kalman Filter (LETKF) and the Stony Brook Parallel Ocean Model (sbPOM). The LETKF is able to represent small scale variations effectively. We assimilated the observation data including in two satellite SST data sets (Himawari-8 and GCOM-W/AMSR2) provided by JAXA. The Himawari-8 data allow spatio-temporally high resolution but could include cloud noise. On the other hand, GCOM-W/AMSR2 provides relatively coarse resolution cloud-free data.

In attached figures, we show the satellite and analysis SST distributions and the vertical temperature distributions represented by analysis data along 139E, from November 22 to November 25, 2016. A cyclone passed south of Japan from November 23 to 24, and it snowed around Tokyo with cool air coming southward. The analysis data reproduce the observed SST drop caused by the weather disturbances and reasonably estimate the SST states in the cloudy area and nearshore region missed by the satellite observation. Also, subsurface isotherms became sparse along 139E, suggesting the mixed layer deepening induced by the cyclone.

We are constructing a web site to operationally provide the information for fishery applications. The contents include 'analysis data', 'forecast data', 'satellite SST', 'sea levels on observation sites', and 'time series at mooring sites off Kochi'. We are updating the information on the website every week.

In the presentation, we will discuss usability of the satellite SST data for data assimilation in detail.

Keywords: Himawari-8, AMSR2, ocean data assimilation, LETKF, sea surface temperature

Vertical SST variation along 139°E
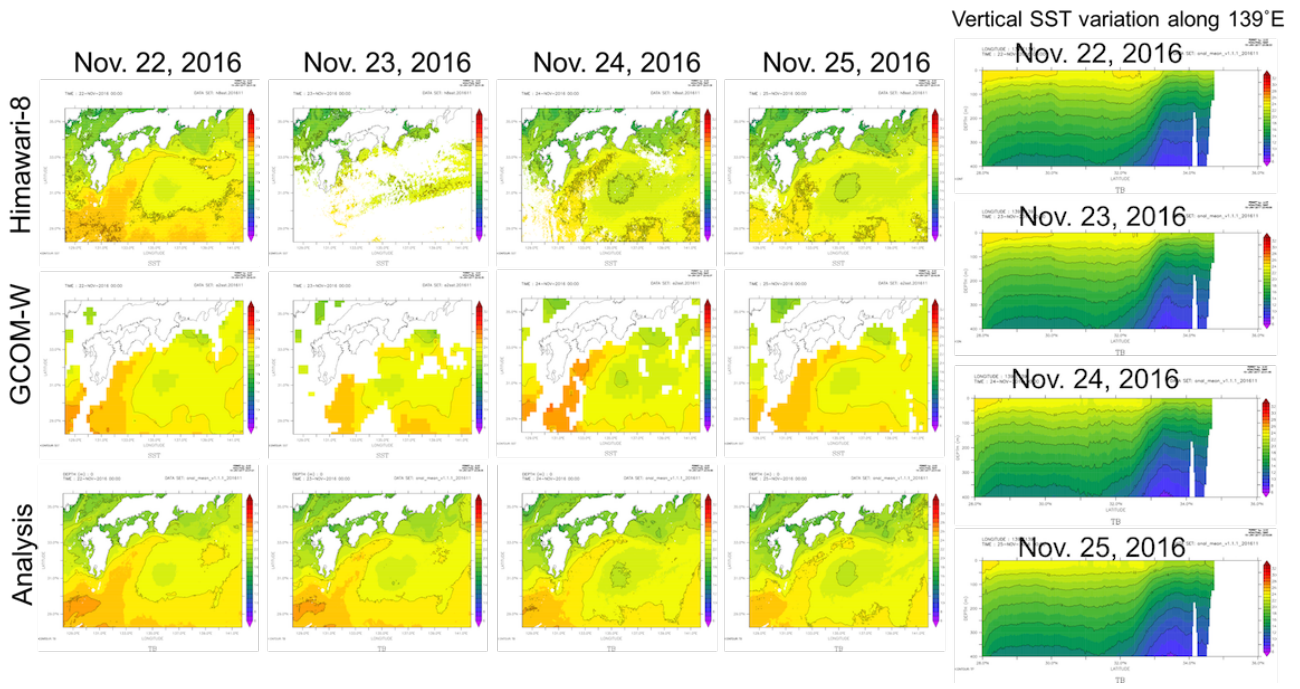
Preliminary results of observing system simulation experiment (OSSE) for future space-based Doppler wind lidar

*Kozo OKAMOTO[1,2], Toshiyuki Ishibashi[1], Shoken Ishii[2], Philippe Baron[2], Kyoka Gamo[4], Taichu Tanaka[1], Takuji Kubota[3]

1. Meteorological Research Institute, 2. National Institute of Information and Communications Technology, 3. JAXA, 4. FUJITSU FIP Corporation

Space-based Doppler Wind Lidar (DWL) can provide global wind profiles that are significantly beneficial for the numerical weather prediction. The feasibility of DWLs has been investigated using OSSE. Our DWL OSSE features a realistic simulation of Lidar scattering from 3-dimentional, hourly aerosol that is consistent to wind field and created by a full-brown lidar simulator. The aerosol is produced by a global aerosol chemical transport model developed by MRI in which wind field is nudged with pseudo-truth. The pseudo-truth atmospheric field is generated from the Sensitivity Observing System Experiment (SOSE) approach. Simulated line-of-sight wind speeds are assimilated with the four-dimensional variational (4D-Var) scheme based on the operational global data assimilation system at JMA. We have conducted OSSEs for DWL onboard a satellite in a polar and low-inclination orbiting satellite, showing forecast improvement by assimilating DWL with inflated observation errors. The preliminary results from the two measurement strategies will be presented.

Keywords: data assimilation, OSSE, Doppler wind lider (DWL), global numerical weather prediction

Global analyses of cloud fraction and cloud phase by using spaceborne-lidar

*Shuichiro Katagiri[1], Kaori Sato[1], Hajime Okamoto[1]

1. Kyushu University

Information of vertical cloud distribution is crucial for the evaluation of the General Circulation Models (GCMs). There were large varieties in the vertical distribution of low-level clouds sorted by pressure and lower tropospheric stability among the models (Watanabe et al., 2011), while retrieved cloud properties from satellites were not converged. Cesana et al. (2016) evaluated three global cloud phase products using the CALIPSO, and showed large differences among the products. In this study, we revisit cloud detection by space-borne lidar.

We modified our cloud mask algorithm originally developed in Hagihara et al (2010) to increase detectability of optically thick low-level clouds. We use the attenuated total backscattering coefficient at 0.532 μm for the discrimination the cloudy pixels with the threshold total backscattering coefficient determined by Okamoto et al. (2007) and Okamoto et al. (2008). Remaining noise is estimated by using the data obtained at an altitude of 40 km to avoid contamination of PSCs.

In this algorithm, identification of the fully attenuated pixel is newly introduced. The discrimination confirms whether no cloud is in the atmosphere or no information is received. The fully attenuated mask is determined by referring to whether the surface return can be detectable or not.

After this cloud mask algorithm is applied, we use the cloud phase discrimination algorithm made by Yoshida (2010), which uses the relation between the depolarization ratio at 0.532 μm and the ratio of two successive attenuated backscattering coefficients at 0.532 μm in vertical, as proxy of extinction coefficient, to distinguish ice and water particles. Here we rely on the following different scattering properties of water and ice clouds. In case of spaceborne lidar observations, depolarization ratio of water clouds is often comparable to that of ice clouds so that the discrimination between ice and water is not possible by depolarization ratio alone. In turn, water clouds generally show larger extinction coefficients than ice clouds for the same depolarization ratio so that the discrimination become possible by using extinction and depolarization ratio. These characteristics are used in the cloud phase discrimination algorithm.

We will show the global analyses of cloud fraction and water/ice fraction by application of the new cloud mask scheme and differences for the old and new schemes are discussed.

Keywords: cloud, lidar

Studies on horizontal scale, vertical scale, and microphysical properties of convective cloud in tropical Pacific by using Cloud Object analysis method

*Naoya Takahashi[1], Tadahiro Hayasaka[1]

1. Tohoku University

Deep convective cloud is important for modulating climate, radiation budget, and hydrological cycle. In the tropics, the mean radiation budget is significantly affected by the amount of upper-level ice clouds associated with deep convective cloud. The objective of this study is to understand the vertical structure and microphysical characteristics of deep convective clouds. In this study, we used the cloud object analysis method which is introduced in Bacmeister and Stephens (2011). This method evaluates horizontal and vertical scale of cloud by using dataset with active sensors on board satellite. Compared with previous studies, we improved the method by using not only CloudSat satellite but also CALIPSO (Cloud-Aerosol Lidar and Infrared Pathfinder Satellite Observations) satellite. The improved method showed that optically thin cirrus has a significant impact on horizontal and vertical scale of deep convective clouds. Moreover, we took advantages of ice cloud properties retrieval from the CloudSat 2C-ICE product to provide microphysical properties of convective core or anvil part in deep convective cloud. We analyzed only deep convective clouds in tropical Pacific oceans (30˚S-30˚N) and used dataset from 2007 to 2011.

From the comparison horizontal and vertical scale of cloud in western tropical Pacific (WP) and that in eastern tropical Pacific (EP), we found that both horizontal and vertical scale in WP are larger than that in EP. However, ratio of width of convective core to entire horizontal scale of deep convective cloud in WP and EP are almost same. Convective activity in WP and EP are different because of difference in sea surface temperature. It suggested that convective activity has an impact on entire horizontal scale of deep convective clouds.

For evaluation of cloud microphysical properties in the convective core and anvil parts, we investigated vertical distribution of cloud particle effective radius and ice water content in each part. Below 15 km, ice cloud particle effective radius and ice water content of convective core part are larger than that of anvil part. This result seems to reflect the process of formulation of deep convective clouds.

Keywords: Deep convective cloud, Cloud microphysics, CloudSat, CALIPSO

Evaluation of Advantages in GCOM-C Polarization Observation for Estimating Aerosol Optical Thickness

*Risa Miyazaki[1], Hiroshi Murakami[1], Masahiro Hori[1]

1. Japan Aerospace Exploration Agency

GCOM-C (Global Change Observation Mission -Climate) satellite, which is equipped with SGLI (Second generation GLobal Imager) sensor, is planned to be launched in the end of this year. It is designed to conduct optically-based measurements for monitoring global environmental change. The SGLI instrument has three major features: (1) global observation covering wavelengths from 380 nm to 12 μm, (2) 250 m spatial resolution for land and coastal areas, (3) polarization /multidirectional observations and near ultraviolet observation. With these features, GCOM-C will be able to provide many products covering a broad range of topics: land, atmosphere, ocean, and cryosphere. It is especially expected to enable to retrieve land aerosol by polarization (PL: 673.5 and 868.5 nm) and ultraviolet (UV: 380 nm) observations with higher accuracy than by the traditional method using blue and red bands because PL and UV observations have little dependeny on the surface reflectance unlike the traditional one.
In this study, we examined the advantage in the PL and UV observations of SGLI for the estimation of aerosol optical thickness (AOT) over land compared with the traditional method using the radiance at 443 and 673.5 nm.
Our method to evaluate the accuracy of estimated AOT by each method is described below. Monthly AOT and mode radius of aerosol of MODIS L3 products (MYD08_M3) are used as a benchmark. Then, radiance at the top of atmosphere (TOA) is calculated by the results of the radiative transfer model (PSTAR3, [Ohta et al., 2010]) for these input data. The surface reflectances of each wavelength is also estimated by using a month's radiation data of POLDER with the assumption that the minimum of the radiance at 490 nm has information of a clear day. We retrieve the AOT and the mode radius from the radiance of TOA considering the observation accuracy (=SNR) of SGLI and the estimation error of the surface reflectance. In this preliminary work, the aerosol type is fixed as the tropospheric aerosol, which is defined as mixture of a water-solble (0.7) and a dust-like (0.3) aerosol. The accuracy of estimated AOT is evaluated by the deviation from the benchmark AOT. We perform these procedures with both the PL + UV method and the traditional one.
As a results, the accuracy of the estimated AOT improved roughly 10 % by using the method of PL+UV compared the traditional one especially in high surface reflectance areas such as the Sahara desert. This would be because the effect of the estimation error of surface reflectance in the AOT accuracy is considerably large at the high reflectance area. In this presentation, we are going to show the dependency of the estimated AOT accuracy on the geometric condition, the benchmark AOT and its mode radius.

Keywords: GCOM-C, SGLI, Polarization observation, Aerosol optical thickness

satellite view of the widespread haze pollution in China

*Liangfu Chen [1], Minghui Tao [1], Zifeng Wang [1]

1. RADI

During the last decades, large increase in anthropogenic emissions has led to severe air pollution problems in China, with high concentration of fine particles and widespread haze layers in many areas. The complex sources and high emissions of atmospheric pollutants has exerted great challenge on air quality in China. Compared with regular measurements in ground sites, satellite observations can provide a unique view of the amounts of atmospheric components and formation processes of haze pollution from regional to global scales. Considering the special atmospheric conditions of high aerosol loading and large spatial and temporal variations in China, we made several improvements such as identification of haze areas in the retrieval of aerosol loading. In particular, we conducted comprehensive investigations in optical properties, spatial variation, and formation processes of the regional haze pollution of China using integrated satellite observations, ground measurements, and meteorological data.

Keywords: air quality , satellite , China

Application of ground observation data in next GSMaP Gauge algorithm

*Tomoaki Mega[1], Tomoo Ushio[1]

1. Graduate School of Engineering, Osaka University

The map of global precipitation amount is one of the important information. The ground-based observation, however, does not cover all Earth. Developed countries operate radar network and rain gauge. Although some developing country installed a few rain gauge or some radars, any developing countries cannot operate radar network and high-density rain gauge network continuously and distribute observation data on time. Observation area of a radar or a rain gauge is local. Development and launching of satellite is expensive. However, characteristic of space-borne observation is to cover whole earth and stable condition.

JAXA is developing and providing near real time global rainfall maps (GSMaP) using the combined Microwave infra-red algorithm with some low orbit satellites. Estimation precipitation by remote sensing of passive microwave radiometer (PMR) is difficult over land. PMR estimation has larger error than ground-based observations. Gauge adjustment GSMaP (GSMaP Gauge) algorithm reduces errors by daily rain gauge. GSMaP Gauge estimated precipitation by precipitation model and daily rain map. Thus quality of GSMaP Gauge depend quality of daily rain map. Available rain gauge map is not uniform quality, because rain-gauges, which real time the map use, are limited number in time.

The plan of the future GSMaP Gauge is to use ground data before the time. The future GSMaP Gauge algorithm uses these data for estimation of the rain model parameters. In no observation area the algorithm interpolate model parameter around ground observation area. The model parameters can improve estimated rain. We will introduce to apply the various ground data in the GSMaP Gauge algorithm.

Keywords: precipitation, satellite

Seasonal and regional dependence of rain estimation from the Himawari-8

*Hitoshi Hirose[1], Atsushi Higuchi[2], Tomoaki Mega[3], Tomoo Ushio[3], Munehisa Yamamoto[1], Shoichi Shige[1], Atsushi Hamada[4]

1. Department of Science, Kyoto University, 2. CEReS, Chiba University, 3. Department of Engineering, Osaka University, 4. AORI, The University of Tokyo

Rain observation with microwave radiometer satellites is essential to make global rain observation data with high temporal resolution. However microwave satellites cannot cover the global area since the number of them is limited. When all microwave satellites are unavailable, utilization of geostationary meteorological satellites (GMS) with high temporal resolution may lead to improvement of rain estimation. Kühnlein et al. (2014) reported that they could estimate rain with high temporal resolution same as GMS by using a statistical method called Random Forest (RF). The machine learning method associates 10 channels information of brightness temperature observed from METEOSAT Second Generation (MSG-2) GMS to rain observation from ground-based radar in Germany. In this method, first some channels are selected randomly from GMS observations to make a small learning sample for rain / no rain classification, called a classification tree. Then the number of tree is increased in the same way, and finally rain / no rain result is classified by majority of all tree's results. In addition rain type classification and rain rate estimation are possible in the RF method. In previous study, analysis area was limited in Germany due to the limit of ground-based radar observing range, but this study applied the RF method to the third generation GMS, Himawari-8, which can cover the East Asia region widely. Moreover we used precipitation radar of the Global Precipitation Measurement (GPM) main satellite instead of the ground-based radar used by the previous study for the truth of rain. As a result we can estimate rain only from satellite observation and expanding the analysis area to not only mid-latitude region but also tropics.

As compared with Europe region in the previous study, the East Asia region analyzed in this study has various seasonal changes. Therefore this study analyzed seasonal and regional dependence of accuracy in the Himawari-8 –GPM rain product. As a result, accuracy of rain area estimation was higher in JJA including rainy season, and was lower in DJF including snowfall. Accuracy of rain rate estimation was higher in MAM and SON including frontal rain, but was lower in JJA including frequent heavy rain and JDF including snowfall. Moreover we applied the machine learning only in sub-tropic region, and then accuracy of both rain area and rain rate estimation was most high, this result suggested that it was important to limit the learning sample into particular rain system for improvement of rain estimation. In the sub-tropic ocean or summertime land region, Himawari-8 –GPM rain product can detect very smaller rain than a few km scale which is difficult to detect by microwave sensor of the GSMaP. This result shows an advantage of high spatial resolution of the Himawari-8 –GPM rain product.

Himawari-8 GMS data is released from the Center for Environmental Remote Sensing, Chiba University. We used near surface rain observed by GPM (Ku PR) and rain intensity observed by ground-based radar in the Japan Meteorological Agency as the truth of Rain

Keywords: Himawari-8, GPM, machine learning, rain estimation

Variability of Vertical Structure of Precipitation over Sumatra and Adjoining Oceans from Long-Term Measurements of TRMM PR

*Marzuki Marzuki[1], Hiroyuki Hashiguchi[2], Mutya Vonnisa[1], Harmadi Harmadi[1], Ovandriyove Ovandriyove[1], Elfira Saufina[1]

1. Department of Physics, Andalas University, 2. RISH, Kyoto University

This study is a follow-up of a previous study on the vertical structure of precipitation over Sumatra [1]. Spatial, seasonal and diurnal variabilities of the vertical structure of precipitation have been studied using 17 years of Tropical Rainfall Measuring Mission's Precipitation Radar (TRMM PR) version 7 data over Sumatra and adjoining oceans. Special emphasis has been put on six different climatic rain regimes, namely, Indian ocean (2 locations), coastal (1 location) and inland (3 locations). The data are classified into different types of precipitation (stratifrom, deep and shallow) including the virga rain. The vertical structure of precipitation over the inland area is compared with long-term measurement of 1.3 GHz Boundary Layer Radar at Kototabang, west Sumatra. The latest TRMM 2A-23 and 2A-25 products (version 7) have been statistically analyzed. First, the spatial, seasonal, and diurnal variations of storm height and freezing level have been investigated. It is found that tall storm is more dominant over the inland than coastal and ocean. Same trend is also observed for melting level height. However, the coastal area has lower percentage of tall melting layer than inland and the ocean. Second, mean vertical profile of radar reflectivity (VPR) has been studied for the stratiform and convective precipitation. The VPR variability has been analyzed for different seasons and diurnal cycles as well as rain intensities. Third, the characteristics of rain intensification and weakening in the vertical direction have been examined by the statistical analysis of VPR gradient (VPRG) above and below the melting layer. Detailed information about the result will be presented during the meeting.

[1] Marzuki, Hashiguchi, H., Kozu, T., Shimomai, T., Shibagaki, Y., Takahashi, Y., 2016, Precipitation Microstructure in Different Madden–Julian Oscillation Phases over Sumatra, Atmospheric Research, Vol. 168, pp. 121-138.

Keywords: vertical structure of precipitation, TRMM PR, Sumatra

Relationships among Vertical Structure of Precipitation, Lightning and Hydrometeor Characteristics along the Equatorial Indonesia

*Marzuki Marzuki[1], Hiroyuki Hashiguchi[2], Mutya Vonnisa[1], Harmadi Harmadi[1], Elfira Saufina[1]

1. Department of Physics, Andalas University, 2. RISH, Kyoto University

In a previous study [1], we have investigated the regional variability of raindrop size distribution (DSD) along the equator through a network of Parsivel disdrometers in Indonesia. Fourth disdrometers were respectively installed at Kototabang (KT; 100.32 E, 0.20 S), Pontianak (PT; 109.37 E, 0.00 S), Manado (MN; 124.92 E, 1.55 N) and Biak (BK; 136.10 E, 1.18 S). We have found that the DSD at PT has more large drops than at the other three sites. The DSDs at the four sites are influenced by both oceanic and continental systems, and majority of the data matched the maritime-like DSD that was reported in a previous study. Continental-like DSDs were somewhat dominant at PT and KT. The differences in the DSD for the four sites may indicate the difference in characteristics of microphysical process accompanying the formation and evolution of DSD at each location which may be related to the variability of topography, mesoscale convective system propagation and horizontal scale of landmass. However, a detailed investigation regarding this hypothesis has not been yet conducted. Therefore, this work tries to overcome such issue by studying the relationship among the vertical structure of precipitation, lightning and the DSD at the fourth locations. The 17 years of latest Tropical Rainfall Measuring Mission's Precipitation Radar (TRMM PR) (version 7) products are statistically analysed to investigate the characteristics of vertical structure of precipitation at each location. The World Wide Lightning Location Network (WWLLN) data are used to study the lightning characteristics at each location. Detailed information about the result will be presented during the meeting.

[1] Marzuki, M., Hashiguchi, H., Yamamoto, M. K., Mori, S., and Yamanaka, M. D.: Regional variability of raindrop size distribution over Indonesia, Ann. Geophys., 31, 1941-1948, doi:10.5194/angeo-31-1941-2013, 2013.

Keywords: vertical structure of precipitation, Equatorial Indonesia, Raindrop size distribution

Validation of GSMaP using ground snowfall observation data

*Yuki Kaneko[1]

1. Japan Aerospace Exploration Agency

The Global Satellite Mapping of Precipitation (GSMaP) is a global rainfall map based on a blended Microwave-Infrared product and has been developed in Japan for the Global Precipitation Measurement (GPM) mission. GSMaP is the product of an hourly global rainfall map in 0.1-degree latitude/longitude grid and available 3-day after observation through the "JAXA Global Rainfall Watch" web site (http://sharaku.eorc.jaxa.jp/GSMaP).

The latest GSMaP version 04 (algorithm version 07) was released in January 2017 to the public. This product gives snowfall retrieval algorithm for the first time using passive microwave instruments that have higher frequency channels. This algorithm apply the rain/snow discriminant technique developed by Prof. Liu (Sim and Liu 2015, Liu and Seo 2013). The new input data of Multisensor Snow/Ice Cover Maps provided by NOAA/NESDIS make suppress the fake precipitation signals in high latitude area (Kubota et al., in preparation).

This research validates the snow retrieval on GSMaP with the AMeDAS dataset provided by Japan Meteorological Agency(JMA) . The uncertainties of ground observation for snow precipitation amount have been well known. It is often influenced significantly of local climate conditions and small differences in measurement.. JMA mainly uses three types of rain gauge, but those observational errors largely depend on the rain gauge type. Addition to this the effect of the wind is negligible especially for snow observation. WMO suggested the method of double fence interconparison reference (DFIR), but even the DFIR requires the data correction when the wind speed at gauge height is over 6 m/sec.

Thus at first the categorical validation using GSMaP and AMeDAS data and its dependency for the condition such as altitude of the observational site and wind speed. Then the precipitation amount of GSMaP is compared with of on the ground which is corrected by the several methods which suit on the rain gauge types.

The objective of this research is to estimate the accuracy and correlation between the snowfall retrieval from satellite observation and ground measurement.

Keywords: GPM, GSMaP, Solid Precipitation

Estimate performance of Global Satellite Mapping of Precipitation and influence of wind on the performance

*Masato I. Nodzu[1], Jun Matsumoto[1], Long Tuan Trinh[1], Thanh Ngo-Duc[2]

1. Tokyo Metropolitan University, 2. University of Science and Technology of Hanoi

1. Introduction

Hanoi urban area, the northern center of Vietnam, is located in the Red River Delta. The growing urban area is faced with the vulnerability by floods. The purpose of this study is to obtain basic knowledge to improve the realtime hydrological forecast system. We examined estimate performance (EP) of Global Satellite Mapping of Precipitation (GSMaP; Aonashi et al. 2009; Ushio et al. 2009) and wind influence on the EP on heavy-rain days.

2. Data and Method

We used daily precipitation of GSMaP RNL version 6 in 2001–2007. Vietnam Gridded Precipitation (VnGP; Nguyen-Xuan et al. 2016) was used to validate the GSMaP precipitation as the ground truth. The both data have a resolution of 0.1 degrees. Utilized wind profiles were what operationally observed with rawinsonde at Hanoi. Analyzed months were May, June, July and August with daily precipitation over 3 mm day^{-1} (Nguyen-Le et al. 2015) and dominant westerly winds in the lower troposphere (Nguyen-Le et al. 2014) almost all over North Vietnam at climatology. The 4 months had most of heavy-rain days with precipitation larger than 50 mm day^{-1} over North Vietnam. A rectangle region including the Lo River basin, one of the Red River branch, is chosen as a reference region. We analyzed heavy-rain days with at least one grid over 50 mm day^{-1} in VnGP. GSMaP EP was defined as a ratio of precipitation in GSMaP to that in VnGP for both grid and regional mean precipitation.

3. Results

The regional mean precipitation was basically underestimated by GSMaP. Thus, we took a strategy to clarify a reason for underestimate. We defined better and worse estimation (BE and WE) cases as cases with EP from 0.5 to 1.2 and less than 0.5, respectively. Zonal winds were significantly larger in the BE cases than in the WE cases below 500 hPa (Fig. 1). The EP was less than 0.5 in most cases on the days with zonal wind less than 2 m s^{-1} at 700-hPa level (Fig. 2). We compared case-mean EP distribution between the relatively westerly and easterly wind cases (WWC and EWC) at 700-hPa level (Fig. 3). The EP in the WWC was higher over North Vietnam including the reference region than in the EWC (Figs. 3a and b). In the upstream of the Red River, the higher EP region was along the River and the northeastern foot of the Hoang Lien Son Mountains in the WWC (Fig. 3c), while the EP was lower in the southwestern foot. The EP in the WWC is much higher than in the EWC in the downstream of the River. GSMaP even largely overestimated the precipitation in the southward of the Delta. The EP difference between the WWC and the EWC was smaller in the northward than the southward both in the downstream and the upstream. The EP difference was relatively small commonly in the southwestern foor of the mountainous region.

- ACG46-P10 -

4. Discussion and Conclusion

These results imply that relatively strong streams made underestimate over the windward region. It is expected that interaction between the topography and winds affected on the EP through the deformation of the hydrometeor distribution on the horizontal-vertical surface. We will investigate the relation between the hydrometeor distribution and the winds in the next step.

References

Aonashi, K., J. Awaka, M. Hirose, T. Kozu, T. Kubota, G. Liu, S. Shige, S. Kida, S. Seto, N. Takahashi, and Y.N. Takayabu, 2009: GSMaP passive microwave precipitation retrieval algorithm: algorithm description and validation. *J. Meteorol. Soc. Japan*, **89A**, 110–136.

Nguyen-Le, D., J. Matsumoto, and T. Ngo-Duc, 2014: Climatologi- cal onset date of summer monsoon in Vietnam. *Int. J. Climatol.*, **34**, 3237–3250, doi:10.1002/joc.3908.

Nguyen-Le D, J. Matsumoto, and T. Ngo-Duc, 2015: Onset of the rainy seasons over the eastern Indochina Peninsula. *J. Climate,* **28**, 5645–5666, doi: 10.1175/JCLI-D-14-00373.1.

Nguyen-Xuan, T., T. Ngo-Duc, H. Kamimera, L. Trinh-Tuan, J. Matsumoto, T. Inoue, and T. Phan-Van, 2016: The Vietnam Gridded Precipitation (VnGP) dataset: Construction and validation. *SOLA*, **12**, 291– 296, doi:10.2151/sola.2016-057.

Ushio, T., K. Sasashige, T. Kubota, S. Shige, K. Okamoto, K. Aonashi, T. Inoue, N. Takahashi, T. Iguchi, M. Kachi, R. Oki, T. Morimoto, Z. Kawasaki, 2009: A Kalman filter approach to the Global Satellite Mapping of Precipitation (GSMaP) from combined passive microwave and infrared radiometric data. *J. Meteorol. Soc. Japan*, **87A**, 137–151.

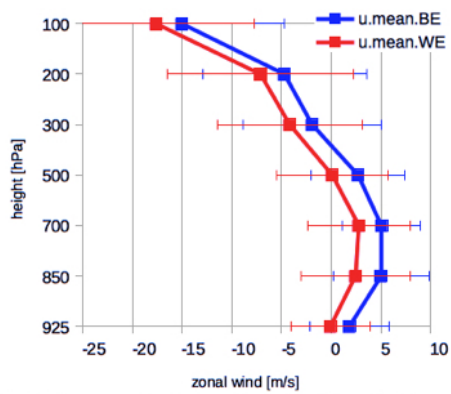Keywords: Orographic rainfall, Asian monsoon

Fig. 1. Mean zonal wind profile in the BE and WE cases in May, Jun, August and September in 2001–2007 at Hanoi.
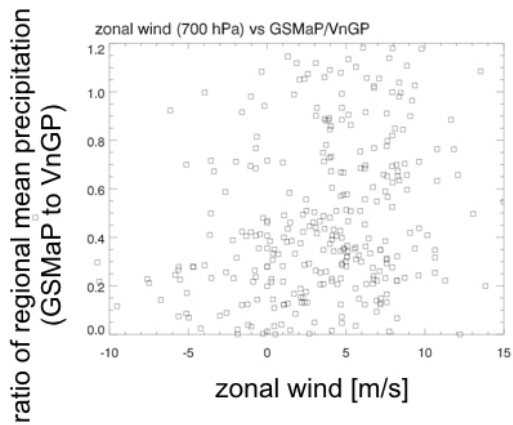

Fig. 2. Relationship between zonal wind at 700 hPa at Hanoi and the estimate performance of regional mean precipitation by GSMaP on heavy-rain days.
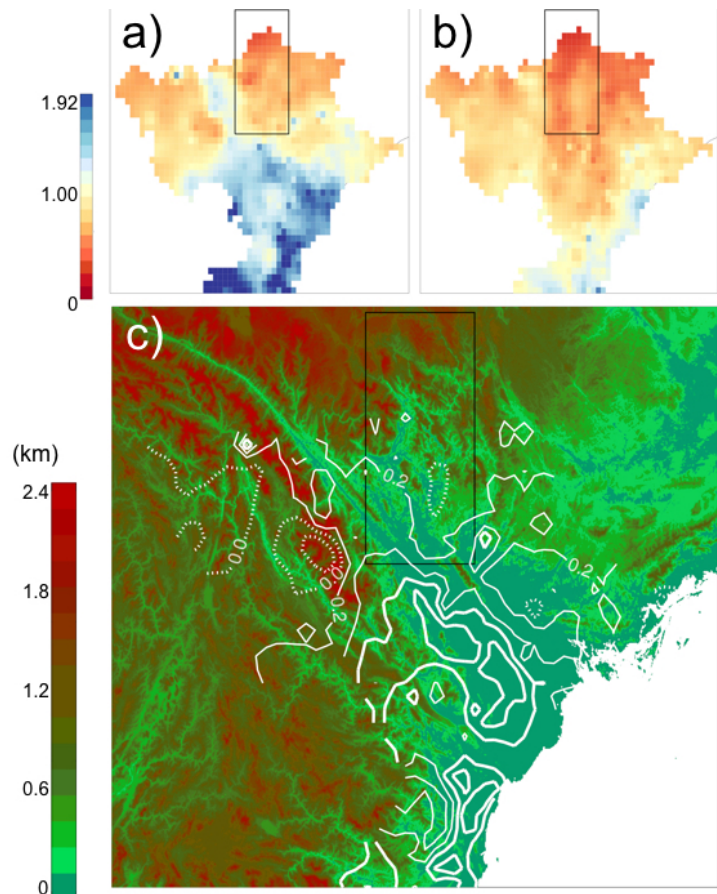

Fig. 3. Estimate performance distribution in the cases of zonal wind (a) over 3.6 m s^{-1} and (b) under 3.6 m s^{-1} at 700 hPa at Hanoi, and (c) their difference ((a) - (b)) shown by solid contours (positive values at interval 0.2, starting at 0.2) and dotted contours (negative values at interval 0.2, starting at 0.0) superposed on the topography map.

Passive microwave rainfall retrievals for tropical cyclones with understanding of microphysical characteristics from cloud resolving models

*Yeji Choi[1], Dong-Bin Shin[1]

1. Yonsei Univ.

Satellite passive microwave observations have been widely used for better precipitation measurements because microwave signals are well associated with the vertically integrated quantities of various hydrometeors in the precipitation system. Understanding the relationships between hydrometeor distributions and radiometric observations is commonly achieved from a-priori information based on cloud and radiation transfer simulations. However, major difficulties in making the a-priori information reside in the simulation variabilities resulted from the assumed microphysical process and insufficient 3-dimensional (3-D) descriptions of radiative signatures as observed by satellite sensors. According to Shin and Kummerow (2003), liquid particle profiles over the precipitation fields can be constructed realistically by matching the radar reflectivity profiles from simulations and GPM dual frequency radar (DPR) observations. However, ice particle profiles produce significant discrepancies in scattering signals depending on the microphysical parameterization methods used in constructing a-priori information. It is then suggested that selecting a proper microphysics scheme showing the most similar microwave signatures for both emission and scattering to the observations can have a substantial impact on the retrieval results. Especially for heavy rainfall systems which can produce large amounts of ice particles, scattering signals should be appropriately described in the a-priori information.
In this study we firstly assessed five microphysical parameterization methods including Thompson, Morrison, WDM6, NSSL-2mom and Thompson aerosol-aware schemes in the Weather Research Forecasting (WRF) model by analyzing the emission and scattering characteristics of each scheme from the perspective of microwave observations for several tropical cyclone cases. Then, the best performed microphysics scheme among them is selected and used to retrieve rain rates. This process may reduce the uncertainties due to the incorrect assumptions on microphysical properties of precipitating clouds. Moreover, as pointed by Kim et al (2016) proper descriptions of the scattering signals along viewing directions can also affect the retrieval quality. We construct more realistic a-priori databases with the 3-D radiative transfer treatment and the best performed microphysics schemes for the GPM microwave imager (GMI). The enhanced prior knowledge is tested to measure the precipitation fields for several tropical cyclone cases.

Keywords: microwave satellite remote sensing, tropical cyclone rainfall measurements, microphysical characteristics of tropical cyclone, microphysics schemes of cloud resolving models

GSMaP RIKEN Nowcast (GSMaP_RNC): an overview

*Shigenori Otsuka[1], Shunji Kotsuki[1], Takemasa Miyoshi[1]

1. RIKEN Advanced Institute for Computational Science

The Japan Aerospace Exploration Agency (JAXA)'s Global Satellite Mapping of Precipitation (GSMaP) provides hourly precipitation estimates over the world except the polar regions. The near-real-time product (GSMaP_NRT) is distributed about four hours after the nominal observation time, whereas the real-time estimate (GSMaP_NOW) is uploaded 30 minutes after the observation time. However, for disaster prevention, short term forecast will add value if available. Otsuka et al. (2016) developed a GSMaP nowcasting system based on space-time extrapolation. The system employs the cross-correlation method to estimate motion vectors of precipitation features, as well as an ensemble Kalman filter to better estimate motion vectors. The system is running stably for more than a year. This year, RIKEN will make the real-time nowcasting products open to public (GSMaP RIKEN Nowcast, GSMaP_RNC). This presentation will provide an overview of the system design and the latest status.

References:
Otsuka, S., S. Kotsuki, and T. Miyoshi, 2016: Wea. Forecasting, 31, 1409-1416.

Keywords: GSMaP, nowcast, data assimilation

Global Drop Size Distribution observed by Dual-frequency Precipitation Radar onboard Global Precipitation Measurement core satellite

*Moeka Yamaji[1], Takuji Kubota[1], Atsushi Hamada[2], Yukari Takayabu[2], Riko Oki[1]

1. Japan Aerospace Exploration Agency , 2. Atmosphere and Ocean Research Institute, the University of Tokyo

Precipitation is one of the most essential parameters in the Earth system. Many places in the world face water problems, such as water shortages and floods. Precipitation observation by rain gauges and ground radars cannot cover overall Earth's surface, and are limited spatially and temporally. It is important for us to observe global rainfall by spaceborne sensors.

Following the success of the Tropical Rainfall Measuring Mission (TRMM) launched in 1997, Global Precipitation Measurement (GPM) core satellite was launched in 2014. GPM core satellite carries Dual-frequency Precipitation Radar (DPR), which consists of the Ku-band (13.6GHz) precipitation radar (KuPR) and the Ka-band (35.5GHz) precipitation radar (KaPR). DPR is expected to have better accuracy for precipitation estimation, relative to single-frequency radar (13.8GHz) used in TRMM, by measuring snow and light rain via high-sensitivity observations from the KaPR, and by providing drop size distribution (DSD) information based on the differential scattering properties of the two frequencies. Furthermore, owing to higher orbital inclination of GPM core satellite (65 degrees) than that of TRMM (35 degrees), DPR is the world's first space-borne precipitation radar observing middle and higher latitudes area.

GPM/DPR level-2/3 (L2/L3) product provides information of the DSD, which is one of the factors that characterizes precipitation but is a main unknown factor of precipitation remote sensing.

Firstly, we confirm the climatology of particle diameter (Dm, [mm]) and particle number concentration (Nw, [m^{-3}]) for 2 years calculated by using GPM/DPR L3 product. Generally, it is found that Dm is larger over land than over the ocean and Nw shows an opposite trend to Dm. In addition, Dm in 20-40 degrees is slightly smaller than other latitudes over the ocean. It is also found that there are seasonal differences in some area, such as Amazon and mid-latitude area. This was consistent with Kozu et al. (2009).

In this study, we use L2 products to analyse in detail by comparing with rain rate. We are planning to apply to the DSD database for Global Satellite Mapping of Precipitation (GSMaP) algorithm in the future.

An experimental study of an Artificial Neural Network (ANN) algorithm to retrieve Precipitable Water (PW) using AHI data

*Yeonjin Lee[1], Myoung-Hwan Ahn[1], Su Jeong Lee[1]

1. Department of Atmospheric Science and Engineering, Ewha Womans University, South Korea

The next Geostationary Korea Multi-Purpose SATellite (GEO-KOMSAT-2A) equipped with the new Advanced Meteorological Imager (AMI), which has improved performance in the spectral (16 spectral bands covering the spectral ranges of 4 visible, 2 near-IR and 10 IR), spatial (2 km at in nadir for the IR channels) and temporal (every 10 min), is scheduled to launch in 2018. It is expected that the finer spatial and temporal distribution of the Total precipitable Water (TPW) product will play an important role in the short-term weather forecast. Current study investigates the possibility of Artificial Neural Network (ANN) approach to retrieve TPW without compensating spatio-temporal resolution of the raw observation data nor the first guess information such as from numerical weather prediction (NWP) model. A multilayer (3 layers; input, hidden and output) perceptron (MLP) feedforward backpropagation algorithm is trained using a training dataset carefully prepared to have general, extensive, and comprehensive representation of real world. The dataset consists of input variables of the simulated Advanced Himawari Imager (AHI) brightness temperatures (9 channels centered at 6.25, 6.95, 7.35, 8.60, 9.63, 10.45, 11.20, 12.35, 13.30 micrometer), 6 dual channel differences, day, time, latitude, longitude, satellite zenith angle and altitude (only land) and the corresponding TPW as output variable. The trained ANN algorithm is applied to the actual AHI data and the results are analyzed to demonstrate the possibility of the ANN TPW for an outbreak of severe convections.

Keywords: Artificial Neural Network, Total Precipitable Water

Development status of the GCOM-W AMSR2 research products

*Nodoka Ono[1], Misako Kachi[1], Takashi Maeda[1], Hiroyuki Tsutsui[1], Mieko Seki[2], Tomoyuki Nomaki[2]

1. Japan Aerospace Exploration Agency, 2. Remote Sensing Technology Center of Japan

The Japan Aerospace Exploration Agency (JAXA) operates the Global Change Observation Mission –Water (GCOM-W) launched in May 2012. The GCOM-W satellite carries the Advanced Microwave Scanning Radiometer-2 (AMSR2). In this mission, eight geophysical values (water vapor, cloud liquid water, precipitation, sea surface temperature, sea surface wind, sea ice concentration, snow depth, and soil moisture) were defined as the standard products, and has been provided to general users since May 2013. Also, research products were defined as a candidate of future standard product in March 2015. Among the standard products, we will update algorithms of sea surface temperature, sea surface wind speed, sea ice concentration, soil moisture content to version 3 in March 2017. As a result of verifying new version products with ground observation and/or other satellite data, accuracy has improved. For example, regarding the sea surface temperature product, we updated the algorithm to change the method of sea surface wind speed correction and conduct more strict quality check to remove inappropriate buoy data, etc. Then, we calculated the root-mean-square-error (RMSE) between the sea surface temperature by AMSR2 and by buoy data provided by National Oceanic and Atmospheric Administration (NOAA). The verification period is from July 2012 to June 2016. Result shows that the RMSE is 0.52 ℃ in new version and improved while that of previous version is 0.56 ℃. In addition, we update the algorithms of research products that are already open to public, 10 GHz sea surface temperature and all-weather sea surface wind speed, and those accuracies are also improved. At the meeting, we will present the detailed verification results of new version of standard products and research products for AMSR2.

Keywords: satellite remote sensing, Water cycle monitoring, Microwave radiometer

Mean Features of Tropical Cyclone Circulation from QUIKSCAT Sea Surface Wind Observations

*Hirotaka Kamahori[1]

1. Meteorological Research Institute

The mean features of vorticity and divergence fields associated with tropical cyclones are evaluated as anomalies from environmental fields, in six tropical cyclone (TC) active basins (the western North Pacific, the eastern North Pacific, the north Atlantic, the north Indian Ocean, the south Indian Ocean, and the South Pacific), using satellite-derived daily sea surface wind observations. A common feature in all basins is that concentric cyclonic vorticity anomalies extend within a 5-degree radius from the TC center with maximum values of 1.5×10^{-4} to 2.0×10^{-4} s^{-1}. The vorticity field near the TC center is the most intense in the North and the South Indian Ocean, and the weakest in the South Pacific. In terms of horizontal size, the radius at the half maximum ranges from 1.8 to 2.4 degree for vorticity fields with the largest in the South Pacific, and the smallest in the eastern North Pacific. In a case of divergence fields, similar results are found with the largest size in the South Pacific and the smallest in the eastern North Pacific. The cyclonic vorticity anomalies in the inner area are surrounded by anti-cyclonic anomalies in all basins, indicating suppression of convective activity due to the tropical cyclones themselves at a large distance from the center. The anti-cyclonic vorticity have maximum values of around 1×10^{-5} s^{-1} and are distributed mainly on the equatorial side of the center. These structures with the cyclonic fields in the inner area and anti-cyclonic fields in the outer area are consistent with the previous study in precipitation fields.

Keywords: Tropical cyclone, Circulation, Sea surface wind

Thermal variability in the South China Sea and its relationship to the western Pacific warm pool

*ChunYi Lin[1]

1. National Museum of Marine Science & Technology

We examine the temperature, heat content, and the size variability in the South China Sea (SCS) connected with the Western Pacific Warm Pool (WPWP), as well as upper-ocean thermal variability in the tropical oceans using satellite data and in situ measurements. Time–frequency–energy distributions, the periods of variability and its trend are extracted by the Empirical Mode Decomposition method and Hilbert–Huang transform method. The increasing rate of mean trend of Western Pacific Warm Pool area is $(2.0\pm0.2) \times 10^6 \, km^2$/decade. Furthermore the warm pool area in the SCS has increased by $(0.2\pm0.03) \times 10^6 \, km^2$ per decade. Observing from the energy of individual component, the semi-annual and annual components forcing from the East Asian monsoon play the main roles on SST variation. Using cross-lag correlation analysis, we demonstrated that the thermal variability in the SCS and WPWP are strongly correlated.

Keywords: South China Sea, Western Pacific warm pool, Thermal variability

Effects of Typhoon and Rainfall on the Kuroshio Surface Temperature and Salinity East of Taiwan

*Chung-Ru Ho[1], Po-Chun Hsu[1], Chen-Chih Lin[1]

1. Department of Marine Environmental Informatics, National Taiwan Ocean University, Keelung, Taiwan

Temperature and salinity are two major variables of the ocean states. Their fluctuations can affect the ocean circulation; moreover, the global changes. In order to understand the effects of wind and rain on the sea surface temperature (SST) and sea surface salinity (SSS) of Kuroshio, we detected the hydrologic characteristics of Kuroshio after heavy rainfall and typhoon passed by east of Taiwan. SST and SSS data are collected from cruises of R/V Ocean Researcher I and spray glider cruises, as well as rain rate data from the Microwave Imager onboard the Tropical Rainfall Measuring Mission. The results show a good correlation between the rain rate and minimum SSS with a coefficient of determination of 0.82 in heavy rainfall cases. The rainfall drops the SSS of Kuroshio with a rain rate of 0.176 psu per mm/hr. Different from the heavy rainfall cases; typhoon not only drops the SST and SSS, but also induces the sub-surface water to uplift. It causes the SSS increases after temporary drops down.

Keywords: Kuroshio, sea surface temperature, sea surface salinity

IoT based visualization service of AMSR2 and GPV in the Arctic Ocean during R/V Mirai cruise MR16-06

*Takeshi Terui[1], Takeshi Sugimura[1], Amane Fujiwara[2], Shigeto Nishino[2], Hironori Yabuki[1]

1. National Institute of Polar Research, 2. Japan Agency for Marine-Earth Science and Technology

Understanding of sea ice situation is the most important issue for vesseles in the sea ice area. In particular, overviewed inforamtion of 1000 km scale is a good indication to determine a safe route. The remote sensing data of sea ice concentration by Earth observation satellites is required. However, limited satelite telecommunication line on the vessel makes on-demand data delivery difficult. And more, if the compressed data would be sent via this line, a professional staff for decoding and visualizing the data must always be needed on the ship. In order to reduce these anxiety and burden, automatical system integrating these processes (delivery, decoding, and visualizing data) is needed. ADS (Arctic Data archive System) has been developed the new integrated system for the ship to delivery and visualize data, which is called VENUS (VEssele Navigator by Unitized Systems). This system was implemented to R/V Mirai cruise MR16-06. In this research, we want to introduce technical performances and advantages of this system.

Keywords: IoT, Raspberry Pi, AMSR2, Ship, Visualization, Automation
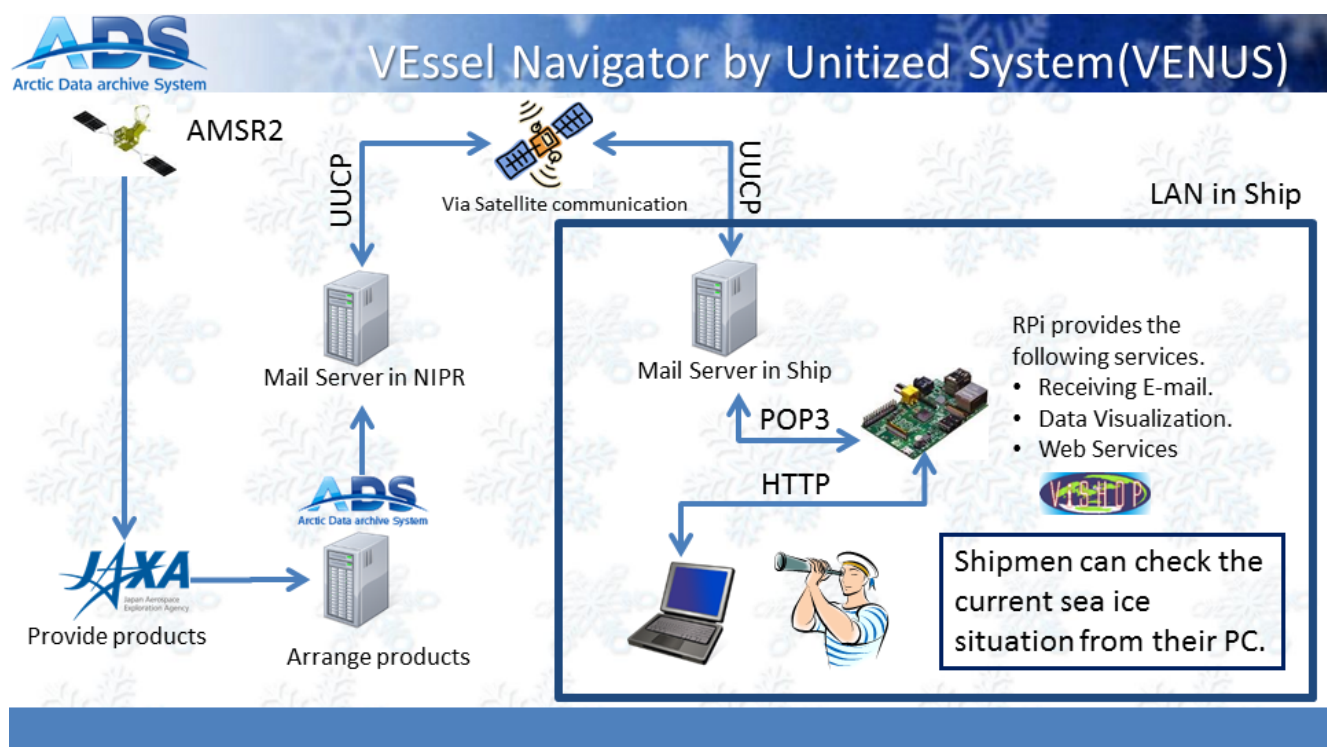
Development of Arctic Route Search System on ADS

*Takeshi Sugimura[1], Takeshi Terui[1], Hironori Yabuki[1], Hajime Yamaguchi[2]

1. National Institute of Polar Research, 2. University of Tokyo

The aim of this study is to build the Arctic Route Search System in order for everyone can easily search optimum navigation route. This system is constructed on ADS (Arctic Data archive System) based on the research products by Arctic Sea Route research group (Yamaguchi laboratory in the University of Tokyo) in ArCS project. In this application, we estimate a sea ice situation and a navigational difficulty from Ice Index based on sea ice concentration and sea ice thickness. A* search algorithm is adopted as search algorithm which select a route with smallest navigation cost among the possible route.
In the present system, because AMSR2 satellite data is used as input condition, route prediction cannot be performed. We are improving the system to use sea ice forecast model TOPAZ4 dataset for input condition, and expect to predict a navigation route for a time period up to 10 days.

Keywords: Northern Sea Route, ADS, AMSR2, TOPAZ4
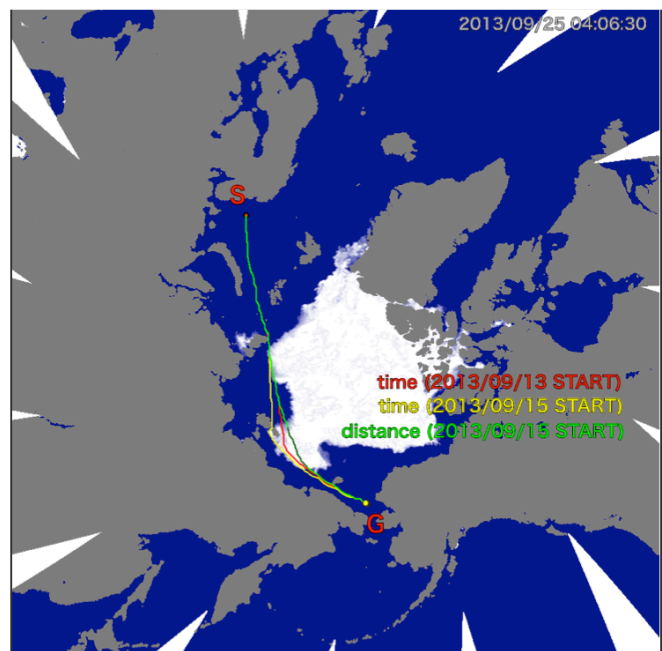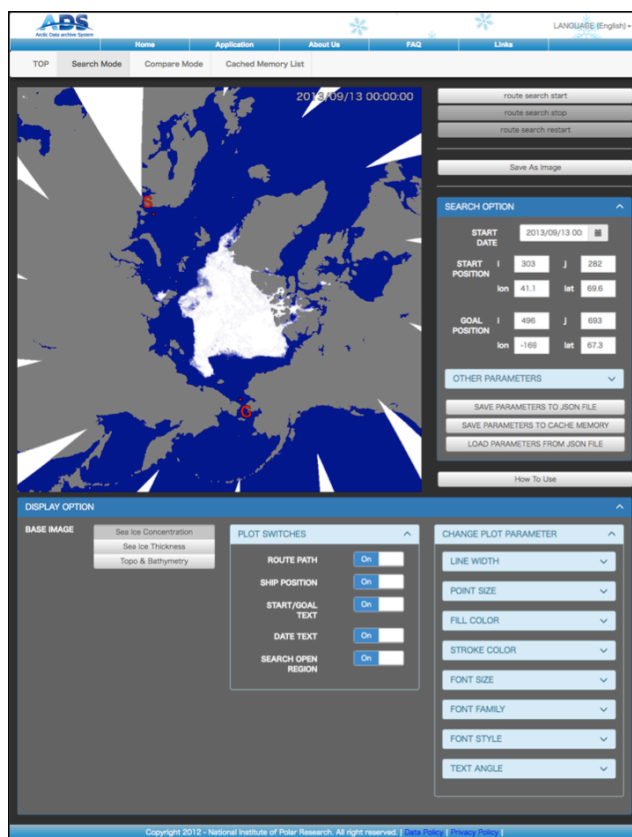
Influence of the sea-ice and cloudiness on the reflectivity over the Southern Ocean

*Alessandro Damiani[1], Raul R. Cordero[2]

1. Chiba University, 2. Santiago de Chile University

The influence of the cloud cover and sea ice concentration (SIC) on the Ultraviolet (UV) Lambertian equivalent reflectivity (LER) at the top of atmosphere over the Southern Ocean has been evaluated for the 1979-2012 period. Despite the high cloud fraction for most of this period, the influence of sea ice was found to be larger than that of cloud cover and it was the main driver of the reflectivity variability. Overall, an increment of the SIC from 0% to 100% resulted in a LER increase of 44 reflectivity units. This value is about twice of the corresponding sea ice-induced reflectivity increase calculated for the observed and modeled shortwave albedo, which is the variable of interest for climate change. On the other hand, cloudiness was found to enhance the UV-LER mostly for low SIC levels. Nevertheless, the analysis was constrained by the difficulty of the passive satellite instruments in identifying cloudiness over high SIC and by the short time series from additional active sensors. Overall, the distribution of the reflectivity for different regions and months shows a marked seasonal-dependent double peak. The reflectivity of the grid-cells characterized by a SIC larger than 30% showed statistically significant negative trends in particularly for the Bellingshausen/Amundsen sea sector. In contrast, the trend of the ice-free grid-cells of the whole Southern Ocean was generally positive.

Keywords: reflectivity, Antarctica, sea ice, cloud fraction

Analyzing Variations of the Kuroshio east of Taiwan using Satellite Altimetry and Hydrographical and Tide gauge data

*Wen-hau Lan[1], Chung-Yen Kuo[1], Chi-Hung Chang[2], C.K. Shum[3], Yuchan Yi[3]

1. Department of Geomatics, National Cheng Kung University, Tainan, Taiwan, 2. Geosensing Systems Engineering and Sciences, University of Houston, Texas, USA, 3. Division of Geodetic Science, School of Earth Sciences, Ohio State University, Ohio, USA

Kuroshio is one of the major currents in the world and plays an important role in the North Pacific climate system due to the sea water, heat and salinity transport and complex air-sea interaction, which is also strongly related to local climate stabilization and natural hazard. In recent years, the velocity of Kuroshio Current increases, attributing to the changes in wind stress over the North Pacific under global warming and affecting sea level along the eastern coast of Taiwan and northward heat transport. Therefore, monitoring of the Kuroshio is of scientific and practical importance. In the study, we focus on the use of contemporary multi-mission satellite radar altimetry and *in-situ* MBT/XBT/Argo to calculate the surface and subsurface (0-2000 *m*) geostrophic velocities and the transport of the Kuroshio east of Taiwan based on the geostrophic balance equation. In addition, we will also analyze interannual and seasonal variations of the Kuroshio transport east of Taiwan using long-term tide gauge data. The estimated current velocities are validated using *in situ* mooring drifters or Argo drift trajectories, and used to study the evolution of the Kuroshio east of Taiwan and the correlation with climate indices, such as the Multivariate ENSO Index (MEI) and the Pacific Decadal Oscillation (PDO) index.

Keywords: Kuroshio Current, Satellite Altimetry , Tide gauge

Improvement of Multi-Altimeter Data by Waveform Classification and Retracking: A case study of Taiwan's wetland

*Wei-Ming Chuang[1], Huan-Chin Kao[1], Chung-Yen Kuo[1], Kuo-Hsin Tseng[2], C. K. Shum[3], Ting-Yi Yang[3]

1. National Cheng Kung University, Taiwan, 2. National Central University, Taiwan, 3. Ohio State University, USA

Satellite radar altimetry becomes an irreplaceable tool to provide accurate surface height measurements over open oceans. However, the accuracy decreases when altimeters approach coastlines or non-ocean surfaces due to the improper geophysical corrections and complex returned waveforms. Many algorithms have been developed for waveform retracking that can improve the accuracy of altimetry data; however, the performance still cannot achieve the same accuracy as that in open oceans. In coastal regions, some waveforms reflected from non-ocean surfaces lead to the worse retracking results. Therefore, waveform classification methods are needed to distinguish waveforms which is truly reflected from ocean or not. Waveform classification used in this study includes two steps. The first step is applying Principal Components Analysis (PCA) to waveforms to extract the features for classification. The second step is using Density-Based Spatial Clustering of Applications with Noise (DBSCAN) to separate waveforms into two groups: ocean and non-ocean waveforms. Then, we remove the non-ocean waveform to improve the accuracy before doing retracking. In this study, we use Jason-2, Envisat and Altika altimetry data over Hsiang-Shan wetland, which is located in Northwestern Taiwan. The satellite-derived results are then evaluated using Hsin-Chu tide gauge data. Finally, we expect building an effective classification method and figuring out the most appropriate retracking algorithm applied for this study area.

Keywords: coastal altimetry, waveform classification, waveform retracking, Hsiang-Shan wetland

The Relationship between the Sea Surface Temperature and Chlorophyll-a in the Global Ocean

*fengchun Su[1], Yung Shiang Lee[2], ChunYi Lin[1]

1. National Museum of Marine Science & Technology, 2. Department of Wealth Management, Hsing-Wu University

The sea surface temperature (SST) and sea surface chlorophyll-a (Chl-a) play important roles in the primary production. However, it is unclear between SST and Chl-a in the ocean. In this study, SST and Chl-a derived from NASA (National Aeronautics and Space Administration) /MODIS (MODerate Resolution Imaging Spectro-radiometer) sensor are gathered from 2001 to 2007. The missing data of SST and Chl-a are filled up by the Data Interpolating Empirical Orthogonal Functions (DINEOF) method. The correlation between SST and Chl-a time series data for each grid is examined. So that a correlation map over the entire global ocean can be constructed to see whether there exists any regional dependence. The results suggest the place of ocean currents and ocean gyres play an important factor between SST and Chl-a. It is found that higher positive correlation area of SST and Chl-a time series is located in most coastal ocean area and where the ocean current flow through. The correlation between the two time series is typically negative correlation in most gyres of ocean. This information could be useful for the study of global changes in sea surface temperature and marine biosphere.

Keywords: Sea Surface Temperature, Sea Surface Chlorophyll-a, Remote-Sensing

The method deriving sea surface temperature - an empirical study on geostationary meteorogical Himawari-8 satellite.

*Yung Shiang Lee[1], ChunYi Lin[2], YuMei Yeh[1], fengchun Su[2], Yu-Hsin Cheng[3]

1. Hsing Wu University, Taiwan, R.O.C., 2. National Museum of Marine Science & Technology , Taiwan, R.O.C., 3. State Key Laboratory of Marine Environmental Science, College of Ocean and Earth Sciences, Xiamen University, Xiamen, China

Sun-synchronous satellites significantly better than geostationary satellites at a time resolution. Recent studies sea surface temperature (SST) mostly as a reference material Moderate Resolution Imaging Spectroradiometer (MODIS). The equatorial region of the tropical Pacific SST bias main factors are wind speed and latent heat in past studies. In this study, deriving the SST in the equatorial region of the western tropical Pacific. Using information from geostationary meteorogical Himawari-8, which data products are level 0. The time span of the data is from July 2015 to December 2016. We apply and compare data mining techniques to improve the quality of Himawari-8 SST. In past study, by a logistic regression approach, it can be determined with an accuracy of $0.4^{o}K$ and an improvement of the correction to 95%.

Keywords: Sea Surface Temperature, tropical Pacific, Wind speed, latent heat

Spatiotemporal variation of vegetation index and sun-induced fluorescence depending on temperature conditions in the Korean peninsula.

*Jae-Hyun Ryu[1], Dohyeok Oh[1], Jaeil Cho[1]

1. Chonnam National University

Current anomalous climate by climate change could cause critical problems in ecology and society. Drought by water deficit and heatwave has been occurred frequently in the Korean peninsula over recent years. Under those abnormal conditions, crop and forest suffered from water and heat stress and they will lead to the decline of crop yield and the weaken ecosystem service. The satellite remote sensing has been applied to monitor the change of vegetation health according to drought event using vegetation indices such as the normalized difference vegetation index (NDVI). Sun-induced fluorescence (SIF) as well as vegetation indices also could indicate the degree of vegetation stress. In this study, the aim is to evaluate the spatiotemporal variations of NDVI and SIF depending on temperature conditions using satellite data in the Korean peninsula. The NDVI from Aqua/Moderate Resolution Imaging Spectroradiometer (MODIS) and the SIF from Meteorological Operational Satellite-A (MetOp-A)/Global Ozone Monitoring Experiment-2 (GOME-2) were used from 2007 to 2016 that these periods include severe drought years. In addition, the MODIS land surface temperature (LST) was used to represent the temperature condition. The seasonal variations of NDVI and SIF were changed according to the degree of drought events, particularly SIF in spring. Also, the value of SIF on August 2016 was dropped comparing the other years due to the critical physiological stress by the worst recorded heat wave. In addition, the increased patterns of SIF or NDVI to LST was clearly shown under the condition less than about 29˚C, and both SIF and NDVI were decreased at higher temperature condition. However, the sensitivities of NDVI or SIF to LST was higher in crop than forest. Further, depending on the regions, South and North Korea, the patterns of NDVI or SIF to LST was different: The forest in North Korea were more sensitively responded than South Korea. Our results represented that NDVI and SIF were useful indicators to detect the heat stress on vegetation and to understand effect of climate.

Keywords: Vegetation index, Sun-induced fluorescence, Temperature, Korean peninsula

Retrieving solar-induced chlorophyll fluorescence from GOSAT measurements with considering radiance offset's dependence on solar zenith angle and observed radiance

*Haruki Oshio[1], Yukio Yoshida[1], Tsuneo Matsunaga[1]

1. National Institute for Environmental Studies

In recent years, satellite remote sensing of solar-induced chlorophyll fluorescence (SIF) has attracted attention as a method for elucidating the photosynthetic activity of terrestrial vegetation. SIF is emitted by chlorophyll molecules: part of the solar radiation absorbed by chlorophyll is not used for photosynthesis and re-emitted as red and far-red radiation. SIF includes information on partitioning of the absorbed solar radiation by chlorophyll. Several studies retrieved SIF from high-resolution spectra in far-red domain obtained by the greenhouse gases observing satellite (GOSAT). The retrieval principle was based on the filling-in of Fraunhofer line by SIF. Non-linearity of the analog circuit in GOSAT spectrometer adds indistinguishable zero-level offset term to SIF. Therefore, the zero-level offset correction becomes important to obtain the SIF accurately.

The zero-level offset can be evaluated from the retrieved filling-in signal (= zero-level offset + SIF) over the vegetation-free areas where the value of SIF is expected to be zero. Previous studies showed that the zero-level offset increases according to the increase of observed radiance. We investigated the zero-level offset for different land covers and locations and found that the zero-level offset relies not only on the observed radiance but also on the solar zenith angle (SZA). Even when the observed radiance was same, the zero-level offset increased according to the decrease of SZA. Therefore, 2-D correction table considering the observed radiance and SZA was prepared for the zero-level offset correction.

Monthly variation of SIF corrected by the present method was compared with that corrected by the previous method. The comparison was conducted for central Africa (woody savanna), southeast USA (evergreen needle leaf), and west Europe (grassland and cropland). The difference was largest for central Africa and smallest for west Europe for almost all month. The maximum difference reached 0.23 and 0.15 mW/m^2·sr·nm for central Africa and west Europe, respectively. Typical monthly averaged SIF ranged 0–1.5 mW/m^2·sr·nm, thus the difference is significant. Furthermore, the difference was largest in summer for southeast USA and west Europe and in spring for central Africa. This study highlights that indispensable attention is required when the value of SIF is directly used and seasonal cycle is compared among locations having different surface cover and latitude.

Keywords: solar-induced chlorophyll fluorescence, GOSAT, photosynthetic production

Satellite observation of internal waves converting polarity in the South China Sea

*Chan Zhang[1]

1. Second Institute of Oceanography, State Oceanic Administration

According to Synthetic Aperture Radar (SAR) imaging mechanism, the oceanic internal solitary waves (ISWs) can be well recognized. In this study, the polarity conversion of ISWs in the South China Sea (SCS) is investigated using 10-years SAR images from 1999 to 2009. It is found that most of the ISWs in SCS are the depression ISWs. However, in region of the continental shelf of the SCS, some elevations ISWs can be identified. In the total of the 500 oceanic internal wave SAR images used in this study, 32 of them exhibit oceanic internal wave polarity conversion.

Moreover, it is found that the elevation ISWs do not show seasonal-locking characteristic. ISWs are found nearly in every season. The bottom topography, hydrological conditions and local thermocline structure which are generally regarded as the conditions for the generation of the elevation ISWs are further explored. Taking the two-layer KdV theory, it is found that ISWs in SCS exhibit a time gap of about 12.4 hours. This time gap is well consistent with the period of local semi-diurnal tide. Our findings thus strongly suggest that the elevation ISWs in SCS can be evolved from the depression ISWs in SCS, which are generally originated from Luzon strait.

Keywords: oceanic internal solitary waves, polarity conversion, depression ISWs

- ACG46-P28 -

Uncertainty Estimation of Soil Moisture Datasets Using Triple Collocation Methods at Mongolian Grassland

Kohei Suzuki[2], *Jun Asanuma[1], Ichirow Kaihotu[3]

1. Center for Isotopes and Environmental Dynamics, University of Tsukuba, 2. Graduate School of Life and Geoenvironmental Sciences, 3. Graduate School of Integrated Arts and Sciences, Hiroshima University

Uncertainties in soil moisture (SM) datasets were estimated at semi-arid grassland in Mongolia by applying the triple collocation methods (TC). Three SM datasets applied to TC are a SM product of AMSR-E, GLDAS with Noah, and the in-situ measurements.
First, in order to demonstrate capability of TC, the uncertainties acquired through TC and a statistical measure are compared. The results showed that the TC uncertainties of AMSR-E are found to be smaller than the root mean squared difference (RMSD) between AMSR-E and the in-situ measurements. This indicates that the latter includes the systematic errors as well as the random errors of AMSR-E and the in-situ, while the TC uncertainties only identifies the random error of AMSR-E. Therefore, it was shown that TC is capable of providing an absolute measure of uncertainties in a SM dataset, unlike other statistical measures such as RMSD.
Further analyses showed that differences of the vegetation amounts expressed in NDVI and difference between ascending/descending observations of AMSR-E do not cause significant difference in the magnitude of uncertainties. This suggests that these factors did not influence uncertainties of AMSR-E. It is also discovered that, in a few cases, TC cannot calculate uncertainties, which may be attributed to a violation of some of the TC assumptions. This is consistent with previous claims that TC is vulnerable to violations of the assumptions. The current findings suggest that the proper selections and pre-processing of the datasets are of significance.

Keywords: Soil Moisture, Satelite Remote Sensing, AMSR-E, Satellite products validation

Downscaling of AMSR2 soil moisture content using multi-satellite land surface variables with regression kriging

*DAEYUN SHIN[1], Daesun Kim[2], Nari Kim[2], Yangwon Lee[2], sunghwa choi[1]

1. KWCI , 2. Pukyong National University

Soil moisture is a primary state variable of hydrology and the water cycle over land. Recent remote sensing technologies have enabled microwave satellite sensors to monitor soil moisture for wide area irrespective of weather conditions. AMSR-E (Advanced Microwave Scanning Radiometer - Earth Observing System) instrument on board the Aqua satellite which was launched in 2002 provided global daily 25-km soil moisture data, and MIRAS (Microwave Imaging Radiometer with Aperture Synthesis) instrument on board the SMOS (Soil Moisture and Ocean Salinity) satellite which was launched in 2009 produces global daily 25-km soil moisture data. Also, AMSR2 (Advanced Microwave Scanning Radiometer 2) instrument on board the GCOM-W1 (Global Change Observation Mission-Water 1) satellite which was launched in 2012 succeeds the role of AMSR-E and provides global daily 25-km and 10-km data. NASA (National Aeronautics and Space Administration) has launched SMAP (Soil Moisture Active Passive) satellite in 2015. It has an active radar and a passive radiometer for producing global daily 3-km and 36-km soil moisture data, respectively, but owing to the failure of the radar, only 36-km data is available now. The spatial resolution of 10 to 36 km is not sufficient for regional-scale applications for hydrology and meteorology although the temporal resolution is quite appropriate. To solve the problem of limited spatial resolution of soil moisture data retrieved from microwave satellite sensors, this study presents the downscaling by spatial statistical methods combined with various land surface variables. To date, statistical methods such as multiple regression and machine learning have been employed for downscaling of soil moisture. However, the inevitable residuals (that is, the part which cannot be explained by the statistical models) bring about differences between the original and the downscaled data, so the consistencies between them may not be maintained. To overcome the drawback, a novel method named regression kriging has been proposed by combining multiple regression and kriging interpolation. Downscaling by the regression kriging can produce a high-resolution data which is spatially consistent with the original data through the correction of residuals. Several studies conducted the downscaling by regression kriging for rainfall datasets such as TRMM (Tropical Rainfall Measuring Mission), but the application of this novel method to soil moisture dataset has not been reported yet. In this study, we carried out the downscaling of AMSR2 soil moisture data using multi-satellite land surface variables with the regression kriging. The database for LST (land surface temperature), RR (rising rate of LST in daytime), NDVI (normalized difference vegetation index), NDWI (normalized difference water index), TVDI (temperature vegetation dryness index), and SA (surface albedo) was built using the satellite images from MODIS (Moderate Resolution Imaging Spectroradiometer) and COMS (Communication, Ocean and Meteorological Satellite). The low-resolution soil moisture data from AMSR2 on the 10-km grid was downscaled on the 1-km grid using the land surface variables. The spatial consistency before and after downscaling was be measured by comparing the pixel values of the low-resolution grid with the upscaled block means of the high-resolution grid. Our results of the spatial consistency showed a correlation coefficient greater than 0.95. The downscaled soil moisture data can be used in various regional-scale applications for hydrology and meteorology.

Keywords: Satellite remote sensing , Soil moisture, Statistical downscaling, Regression kring

The nonlinear three-band algorithm for retrieving land surface temperature from Himawari-8

*Yuhei Yamamoto[1], Hirohiko Ishikawa[1]

1. Disaster Prevention Research Institute, Kyoto University

Introduction

The land surface temperature (LST) is a key parameter of the land-atmosphere interaction on various scales. Since satellite observations can provide LST data over wide area in homogeneous quality, LST retrieval algorithms have been proposed for various sensors. The Advanced Himawari Imager (AHI) onboard Himawari-8, a next-generation geostationary satellite, has three thermal infrared bands in the spectral range 10–12.5 μm, while previous satellites had two. The 10–12.5 μm range is suitable for retrieving LST since the atmospheric absorption is small in this range, and is mainly by water vapor. Another advantage of this range is that the land surface emissivity (LSE) does not differ much among various constituents of the land surface. The retrieval of the LST is sensitive to LSE estimation and water vapor estimation. (Li et al., 2013). Therefore, a retrieval algorithm that has high accuracy and high robustness against the uncertainties in input data is required. We present a new LST retrieval algorithm that makes the maximum use of AHI new window thermal infrared (TIR) bands.

Method

Previous studies (Atitar and Sobrino, 2009; Takeuchi et al., 2012) employed a nonlinear split-window algorithm (NSW), which considers the effect of the atmospheric attenuation by utilizing the differential adsorption of two adjacent TIR bands. In contrast, we have developed a nonlinear three-band algorithm (NTB) by utilizing a combination of AHI three TIR bands. The NTB is inspired from a three-band algorithm (TB) developed by Sun and Pinker (2003) which used two TIR and a near infrared band. The formula of the algorithm includes ten coefficients. The optimum values of these coefficients are derived using a statistical regression method from the simulated data, as obtained by a radiative-transfer model. The simulated data sets include the spectral response functions for the three AHI TIR bands, the seven satellite zenith angles (SZAs) from 0° to 60°, 215 radiosonde profiles, 6 LSTs for each profile, and 86 band LSEs. As a result, 109467 LST –($T_{10.4}$, $T_{11.2}$, $T_{12.4}$) relations were obtained in total for a fixed SZA value. After obtaining the coefficients in this way, we searched the best LST algorithm for five cases: three types of NSWs, one type of TB and one type of NTB.

Results

We checked the root-mean-square error (RMSE) in terms of the SZA, LST and precipitable water (PW) dependence by using dataset used to obtain coefficients. The result showed that the NTB can stably estimate the LST especially in hot and wet environments by comparison to the NSW. Moreover, we evaluated the sensitivities of five LST algorithms to the uncertainties in LSE, PW and noise equivalent delta-temperature (NEdT) by using the validation data independent of dataset used to obtain coefficients. Consequently, it was clarified that the NTB has the highest robustness against the uncertainties in LSEs and NEdTs of three TIR bands. The total estimation error of NTB is about two third of NSW for SZA smaller than 40°. Therefore, it is concluded that the NTB is more suitable for the LST retrieval from AHI than the NSW.

The NTB is combined with an appropriate cloud mask and a LSE products to retrieve LST (see Figure 1 for example). The spatial resolution of the AHI is about 2 km and the observation cycle is 10 minutes. Though the horizontal resolution is inferior to the products from polar-orbiting satellites, the high frequency

observation explores new use of LST products. For example, the AHI can detect a difference in urban area such as commercial, industrial, and residential regions. Hence, it is expected that our Himawari-8 LST product is applicable to studies of thermal property in smaller scales (see Figure 2).

References

Z. Li *et al.*, *Remote Sens. Environ.*, vol. 131, pp. 14–37, 2013.

M. Atitar and J. A. Sobrino, *IEEE Geosci. Remote Sens. Lett.*, vol. 6, no. 1, pp. 122–126, 2009.

W. Takeuchi *et al.*, *Asian J. Geoinformatics*, vol. 12, no. 2, 2012.

Keywords: Land surface temperature (LST), Himawari-8, Remote sensing
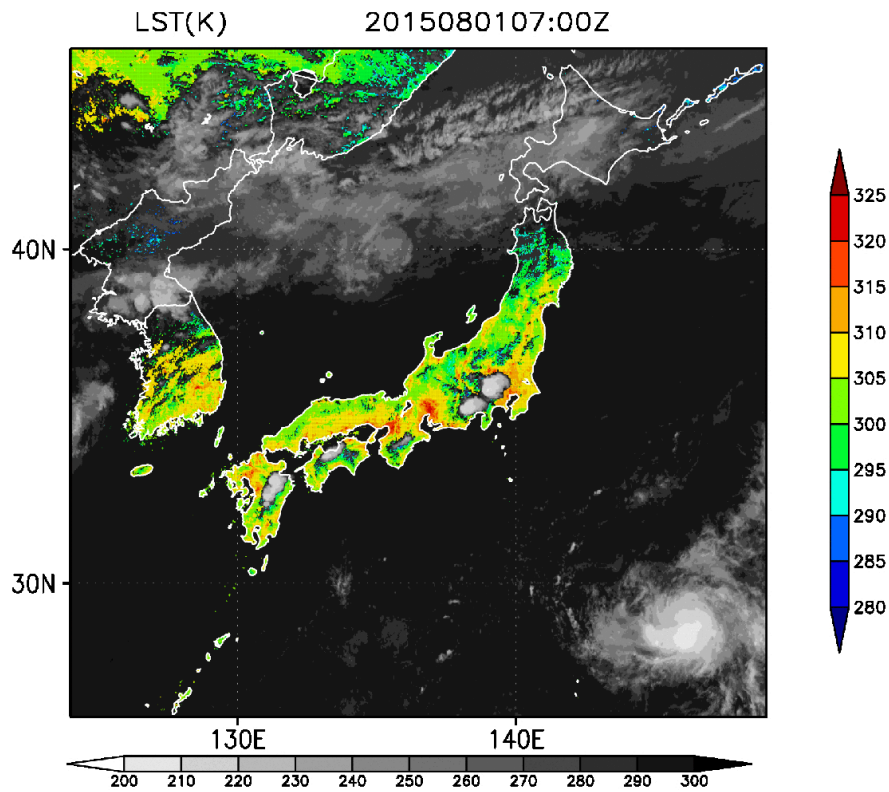
Figure 1. An example of the Himawari-8 LST product over Japan area on 01 August 2015 at 07:00 UTC.
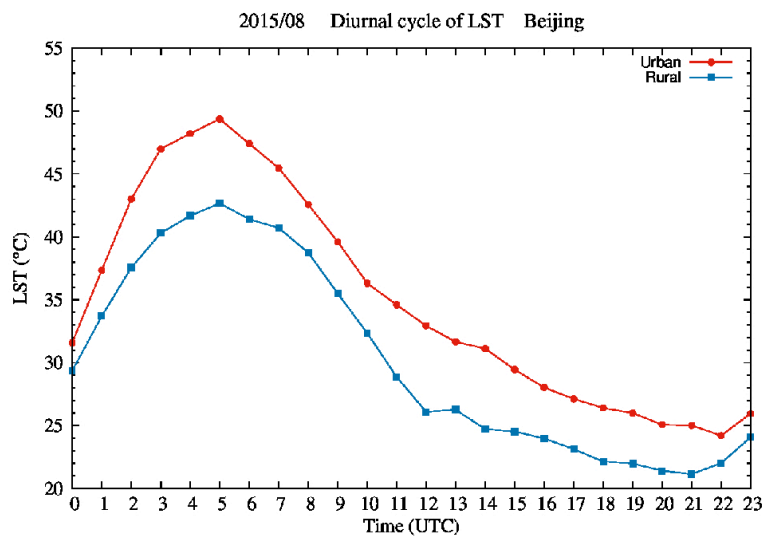

Figure 2. The Diurnal cycle of LST in Beijing urban and rural areas which was generated by composite processing for 31 days in August 2015. The temporal resolution was reduced to 1 hour.

A dynamic approach to retrieving snow depth based on the technology of integrating satellite remote sensing and in situ data

*Liang Zhao[1,2], Yuxiang Zhu[3], Ziniu Xiao[1]

1. LASG, Institute of Atmospheric Physics, Chinese Academy of Sciences, 2. National Climate Center, China Meteorological Administration, 3. CMA Training Center, China Meteorological Administration

Hydrological processes and climate in the extratropics are highly affected by the seasonal snow. Essential characteristics both for hydrology and climatology include snow water equivalent and snow depth. We develop a new approach to dynamically retrieving snow depth based on integration of passive microwave remote sensing and in situ data. First, the snow-cover confidence index is established by use of both the passive microwave remote sensing and in situ data, identifying together the snow cover; second, a new dynamic parameterized scheme (distance weighted method) is developed based on the index. The characteristics of the snow-depth retrieval approach are following: on the one hand, for the difference issue of retrieval coefficients in different spatial-temporal circumstances, a solution is proposed that retrieval coefficients are adjusted according to real-time observed snow depth, being the biggest difference from static retrieval approaches; on the other hand, the advantage of spatial-temporal continuity of the passive microwave remote sensing data has been exploited, being able to retrieving the snow depth with relative high resolution and precision in the west China where few stations are located. The results show that the approach implements the efficient integration of passive microwave remote sensing and observed data, exerts the advantages of different source data, improves obviously the retrieval precision in the west China and the south marginal regions of snow cover in the east China, and solves the question in the old integrating approach that the area of snow cover was always relatively smaller in the west China, amplifying the detectable coverage area of snow depth. In contrast to the static retrieval approach, the dynamic retrieval approach avoids efficiently the question that snow depth was overestimated in mountain regions and underestimated in plain regions, so the snow cover and the snow depth are both more real.

Keywords: Snow depth retrieving, Passive microwave remote sensing, dynamical retrieving

Using radar to measure vegetation water stress

*Tim vanEmmerik[1], Susan Steele-Dunne[1], Nick van de Giesen[1]

1. Water Resources Section, Delft University of Technology, The Netherlands

Vegetation water stress significantly affects agricultural and tropical forest canopies. Water shortages in crops influence plant water dynamics, reduces primary production and might eventually lead to plant death. Tropical forests are essential part of global carbon and water cycle. Continuing drying of e.g. the Amazon rainforest might accelerate climate change through carbon losses and changing land surface energy balances.

In addition to ground measurements, various studies have reported observations of plant water stress using active microwave remote sensing. For example, statistical significant variations in radar backscatter were shown to coincide with the onset of water stress over West Africa [1]. Others were able to link radar backscatter time series over the Amazon to the heavy 2005 drought [2].

Additional in situ measurements in agricultural and tropical forest canopies allow further exploration of the full potential of water stress detection using radar. Novel ground measurements techniques have been used to detect and quantify the effects of water stress in various types of plant canopies [3,4], increasing the understanding of how hydrological and plant physiological signatures of water stress affect radar backscatter. Recent efforts have focused on linking these measurements to radar backscatter time series [5].

This presentation aims to present a journey across scales with respect to vegetation water stress. Measurements of changing plant physiological dynamics on leaf and plant levels are linked to radar backscatter on field and forest scales. We aim to demonstrate new insights obtained using field measurements, and highlight the potential of vegetation water stress detection using radar remote sensing.

References

[1]. Friesen, Jan, Susan C. Steele-Dunne, and Nick van de Giesen. "Diurnal differences in global ERS scatterometer backscatter observations of the land surface." *IEEE Transactions on Geoscience and Remote Sensing* 50.7 (2012): 2595-2602.

[2]. Frolking, Steve, et al. "Tropical forest backscatter anomaly evident in SeaWinds scatterometer morning overpass data during 2005 drought in Amazonia." *Remote Sensing of Environment* 115.3 (2011): 897-907.

[3]. van Emmerik, Tim, et al. "A comparison between leaf dielectric properties of stressed and unstressed tomato plants." *Geoscience and Remote Sensing Symposium (IGARSS), 2015 IEEE International.* IEEE, 2015.

[4]. van Emmerik, Tim, et al. "Dielectric Response of Corn Leaves to Water Stress." *IEEE Geoscience and Remote Sensing Letters* 14.1 (2017): 8-12.

[5]. van Emmerik, Tim, et al. "Impact of diurnal variation in vegetation water content on radar backscatter from maize during water stress." *IEEE Transactions on Geoscience and Remote Sensing* 53.7 (2015): 3855-3869.

Keywords: vegetation, remote sensing, drought

JAXA super sites 500: a large footprint ecological monitoring project for satellite validation

*Tomoko Akitsu[1], Kenlo Nishida Nasahara[1], Tatsuro Nakaji[2], Toshiya Yoshida[2], Nobuko Saigusa[3], Hideki Kobayashi[4], Masato Hayashi[5], Masahiro Hori[5], Yoshiaki Honda[6]

1. University of Tsukuba, 2. Hokkaido University, 3. National Institute for Environmental Studies, 4. Japan Agency for Marine-Earth Science and Technology, 5. Japan Aerospace Exploration Agency, 6. Chiba University

JAXA super sites 500 is a large footprint ecological monitoring project for satellite validation. This project has been started from 2013. Its objective is to obtain representing values of leaf area index (LAI), above ground biomass (AGB), and fraction of absorbed photosynthetically active radiation (fAPAR) within the 500 m ×500 m scale, particularly for validation of the ecological products derived by the Global Change Observation Mission-Climate (GCOM-C) satellite, which will be launched in 2017.

LAI, AGB, and fAPAR are essential information for studies of vegetation productivity and carbon cycle. Therefore, these accurate datasets on global and regional scales are needed to be derived by satellite remote sensing. Generally, these datasets have been produced in a satellite sensor's moderate resolution such as 0.25 km, 0.5 km, or 1 km. To assess their accuracy, in-situ data measured within such spatial resolution is desired. However, such data are rarely available. Accordingly, in previous researches, in-situ data was measured within a smaller area such as 100 m ×100 m and then scaled up to the satellite resolution using higher-resolution imagery. In another case, assuming the larger area was covered with homogeneous vegetation, the in-situ data was directly scaled up to the satellite resolution. However, such scaled-up data includes influences caused by micro-topography and a mixture of different land covers. Thus, the LAI, AGB, and fAPAR products of such satellite sensor's resolution have been difficult to validate.

In order to overcome this difficulty, we initiated a "JAXA Super Sites 500" project. We have established in-situ observation sites on some typical forest types in East Asia, from temperate to cool ecosystems: deciduous needle-leaf forest (DNF), evergreen needle-leaf forest (ENF), and deciduous broad-leaf forest (DBF). Each site has 500 m ×500 m square research plot in flat topography area. We had carried out pilot studies on each site, and will start full-fledged observations after launching of GCOM-C.

The purpose of this study is to compare their observation methods and sampling designs within this scale, and to evaluate the quality of the in-situ data. Basically, we set five 400 m length parallel line-transects at 100 m intervals in each site. LAI and AGB were measured along these lines. Canopy LAI was measured by three methods: It was measured at 20 m intervals on each line by using LAI-2200/LAI-2000 (LI-COR, USA) and fish-eye digital camera. It was also measured by using litter trap. Understory LAI was measured by two methods: It was measured at 20 m intervals by using LAI-2200 and by using harvesting method. AGB was measured by two methods: It was measured at several points by using an improved Bitterlich's method. It was also measured within several fixed plots by using a tree census method. Furthermore, we plan to measure fAPAR by using accurate and stable quantum sensors [*Akitsu et al.*, in press].

Keywords: Satellite validation, Large footprint monitoring, Leaf area index, Above ground biomass, Fraction of absorbed photosynthetically active radiation
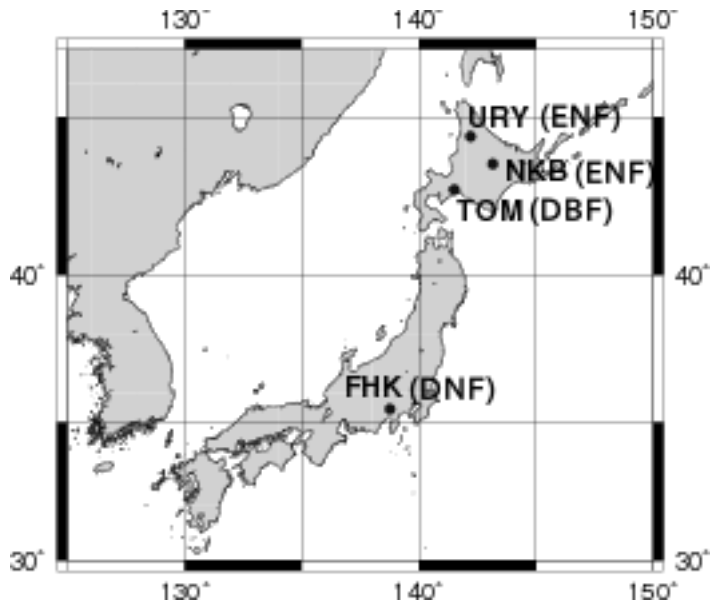
Why Japan's Earth observation has not yet been settled

*Tetsuya Kodama[1]

1. Research Unit I, Research and Development Directorate, Japan Space Exploration Agency

Thirty years have passed since Japan launched its first Earth Obsevation Satellite MOS-1 in 1987.
Due to the introduction of the Information Gathering Satellite Project in 1999, our space program had to suffer heavy staff reduction and budget cuts.
Even after the Basic Space Law was enacted in 2008, the program for the future Earth Observation Satellites is still in a blank state.
In this presentation, a review on the Earth Observation Satellites since the NASDA era and the Task Force Meeting/Remote Sensing Subcommittee (TF) in 2016 together with some proposal for the future program will be presented.

Keywords: Earth Observation Satellite, Space Policy, Decision Making

The potential of GRACE gravimetry to detect fast impoundment of a small reservoir in the upper Yellow River

*Shuang Yi[1], Chunqiao Song[2], Qiuyu Wang[4], Linsong Wang[3], Kosuke Heki[1], Wenke Sun[4]

1. Dept. Natural History Sciences, Faculty of Science, Hokkaido University, 2. Department of Geography, University of California, Los Angeles, Los Angeles, CA90095, United States, 3. Institute of Geophysics and Geomatics, China University of Geosciences, Wuhan, Hubei, China, 4. Key Laboratory of Computational Geodynamics, University of Chinese Academy of Sciences, Beijing 100049, China;

Artificial reservoirs are important indicators of anthropogenic impacts on environments, but their gravity effects have been seldom studied. Here, satellite gravimetry Gravity Recovery and Climate Experiment (GRACE) is utilized to detect the gravity effect of the Longyangxia Reservoir (LR) situated in the upper stream of the Yellow River. Heavy precipitation in the summer of 2005 caused the LR water storage to increase 37.9 m in height or 13.0 Gt in mass. Three different GRACE solutions from CSR, GFZ and JPL and three different filters (an anisotropic decorrelation filter DDK4, Gaussian filter and a decorrelation filter) are compared here. In this case, CSR solutions have the highest signal-noise-ratio and DDK4 shows the best ability to reveal the expected gravity signals. We obtained 109 combinations of inundation area measurements from satellite imagery and water level changes from laser altimetry and in situ observations to derive the area-height ratios in the LR, which agrees well with an alternative method based on the digital elevation model. After removing simulated gravity signals caused by mass changes in the LR, the root mean square of GRACE series in the LR is reduced by 31.1%. If the residuals are totally attributed to GRACE errors, the standard deviation of GRACE observation in this study spot is estimated to be 3.1 cm. With an area of 383 km^2, the Longyangxia Reservoir is the smallest signal source reported to be detected by GRACE.

Keywords: GRACE, space gravimetry, gravity of reservoirs, time-varying gravity, reservoir impoundment

Remotely sensed global distribution of debris thermal resistance on glaciers

*Orie Sasaki[1], Yukiko Hirabayashi[2], Shinjiro Kanae[1]

1. Tokyo Institute of Technology, 2. The University of Tokyo

Supraglacial debris is commonly found in high relief mountains and affects glacier melting rate by altering surface reflectivity and conductive heat flux. Several researches therefore developed local glacier models that reflect debris effects. However, there is no global glacier model that includes debris effects in glacier melting process due to limited information about spatial distribution and thermal properties of debris. Here, we present a global distribution data of debris thermal resistance to account for debris effects in global glacier models. We calculated thermal resistance of debris layer at 90m horizontal resolution on a global scale by utilizing ASTER and CERES satellite products in conjunction with meteorological data, excluding Greenland and Antarctica. Result indicated that 16.8% of total glacier area was covered by supraglacial debris, and regional differences are apparent from region to region. When we classified debris into thin debris and thick debris, it was found that thick debris-covered area was larger than thin debris-covered area, with the exception of Svalbard and Scandinavia. Moreover, we assess the possible uncertainties and limitation of our methodology. Although the uncertainties is relatively high, our estimation provides a necessary basis to calculate the debris effects on glaciers on a global scale, which may refine future predictions of glacier meltwater and its contribution to regional water availability and global sea-level change.

Keywords: debris-covered glacier, thermal resistance

Cirrus optical properties analysis based on EarthCARE observation

*Seiko Takagi[1], Makiko Hashimoto[2]

1. Tokai University, Research and Information Center, 2. JAXA

Cirrus clouds play an important role in the energy budget of the Earth-atmosphere system by their effects on the transfer of radiative energy through the atmosphere. Low clouds have a cooling effect on solar radiation by scattering. On the other hand, the high thin cirrus clouds scatter a small amount of solar radiation and absorb a large quantity of outgoing long-wave radiation from the Earth and its atmosphere. The overall effect of the high thin cirrus clouds is heating on the Earth-atmosphere system.

Cirrus clouds are prominent and yet uncertain components in weather and climate studies because of high location and composed of almost exclusively nonspherical ice crystal of various shapes, such as bullet rosetts, plates, and columns. Progress in numerical model of climate change prediction require improved representations of cloud processes and decreased uncertainties in parameterizations of cloud radiation interactions. Cloud parameterizations in numerical climate models need to define the temporal and spatial distributions of high cloud optical properties. EarthCARE (Earth Clouds, Aerosols and Radiation Explorer) is one of the future Earth observation joint mission of Japanese (JAXA) - European (ESA). EarthCARE satellite aims at understanding of the role that clouds and aerosols play in reflecting incident solar radiation back into space and trapping infrared radiation emitted from the surface in order to improve the numerical climate prediction models. The satellite payload is composed of four instruments; an Atmospheric backscatter Lidar (ATLID), a Cloud Profiling Rader (CPR), a Multi-Spectral Imager (MSI), and a Broad-Band Radiometer (BBR). The EarthCARE orbit is sun-synchronous with an altitude of around 393 km and 14:00 mean local time of the descending node. The MSI will provide Earth images over a swarth width of 150 km with a spatial resolution of 500×500 m in 7 spectral bands; one visible (0.67 um), one near infrared (0.865 um) and two shortwave infrared (1.65, 2.21 um) channels capturing reflected solar right on the day-side of the orbit, and three thermal infrared (8.80 10.80, 12.00 um) channels measuring the emitted thermal radiation from the Earth.

We develop an algorithm to derive cirrus clouds optical properties from MSI Level 2 radiance data as a research product of EarthCARE project. In this study, we modified MWP (Multi-wavelength and multi-pixel) method [M. Hashimoto et al., in revision] to derive cirrus clouds optical properties and operation tests of modified algorithm were performed in using MODIS/Aqua radiance data for the first time.

Keywords: EarthCARE, cirrus